

Fundamental limits of quantum error mitigation

Ryuji Takagi,^{1,*} Suguru Endo,^{2,†} Shintaro Minagawa,^{3,‡} and Mile Gu^{1,4,§}

¹*Nanyang Quantum Hub, School of Physical and Mathematical Sciences,
Nanyang Technological University, 637371, Singapore*

²*NTT Computer and Data Science Laboratories, NTT Corporation, Musashino, 180-8585, Tokyo, Japan*

³*Graduate School of Informatics, Nagoya University, Chikusa-ku, 464-8601, Nagoya, Japan*

⁴*Centre for Quantum Technologies, National University of Singapore, 3 Science Drive 2, 117543, Singapore*

The inevitable accumulation of errors in near-future quantum devices represents a key obstacle in delivering practical quantum advantage. This motivated the development of various quantum error-mitigation protocols, each representing a method to extract useful computational output by combining measurement data from multiple samplings of the available imperfect quantum device. What are the ultimate performance limits universally imposed on such protocols? Here, we derive a fundamental bound on the sampling overhead that applies to a general class of error-mitigation protocols, assuming only the laws of quantum mechanics. We use it to show that (1) the sampling overhead to mitigate local depolarizing noise for layered circuits — such as the ones used for variational quantum algorithms — must scale exponentially with circuit depth, and (2) the optimality of probabilistic error cancellation method among all strategies in mitigating a certain class of noise, demonstrating that our results provide a means to identify when a given quantum error-mitigation strategy is optimal and when there is potential room for improvement.

I. INTRODUCTION

Recent advances in quantum technologies have resulted in the availability of noisy intermediate-scale quantum (NISQ) devices, promising advantages of quantum information processing by control of tens to hundreds of qubits [1, 2]. Yet, inevitable noise remains a critical roadblock in their practical use. Every gate has a chance of error, and left unchecked, their accumulation will likely destroy any potential quantum advantage. The conventional means to correct these errors — quantum error correction — demands tens of thousands of qubits and highly stringent gate fidelities [3, 4], making them a poor match for the practical limitations of NISQ devices.

Quantum error mitigation [5–8] provides a promising alternative. Whereas quantum error correction operates by encoding logical qubits within an untenably large number of physical qubits, quantum error mitigation stipulates that we run available NISQ devices many times. Classical processing of these measurement outcomes can then allow an estimate of the desired computational output (e.g., ground state energy of a Hamiltonian in quantum chemistry [5, 9–11]). Surging interest in these techniques has resulted in diverse approaches, such as zero-error noise extrapolation [12–17], probabilistic error cancellation [12, 18–20], and virtual distillation [21–26].

The performance of these strategies is typically analyzed on a case-by-case basis. While this is often sufficient for understanding the value of the methodology in the context of a specific application, it leaves open more fundamental questions. Are these approaches near-optimal, or could there exist a more effective error-mitigation protocol yet undiscovered? What are the ultimate capabilities of all such strategies?

In this work, we ask, *Can the laws of quantum mechanics imply ultimate bounds on the performance of any such error-mitigation protocol?* To address this, we present a framework that encompasses all aforementioned error-mitigation strategies (see Fig. 1) together with universal quantifiers for their performance. We use these to derive fundamental lower bounds on the sampling cost that guarantees a desired accuracy for each quantum error-mitigation protocol, assuming only the laws of quantum mechanics.

Our results place ultimate performance limits of quantum error mitigation in practical scenarios. We illustrate this by showing two immediate consequences: (1) error-mitigating local depolarizing noise within variational quantum circuits — a key application of NISQ processors under a common noise model [9, 27] — requires exponential sampling overhead regardless of the error-mitigation strategy used, and (2) probabilistic error cancellation — a prominent method of error mitigation — is optimal for certain forms of noise, demonstrating that our bounds reveal when existing error-mitigation methods are already optimal and when there is more room for further improvement.

II. FRAMEWORK

General error mitigation — To establish universal performance bounds shared by a broad class of mitigation protocols, we first introduce a general framework for error mitigation. Our premise begins by assuming that the ideal computation involves a quantum circuit U that results in some ψ , followed by measurement in some arbitrary observable A (See Fig. 1A). Our aim is then to retrieve desired output data specified by $\langle A \rangle = \text{Tr}(A\psi)$. In realistic situations, however, there is noise, such that we have only NISQ devices that prepare certain distorted states $\mathcal{E}(\psi)$. The goal of error-mitigation is to use these distorted outputs to estimate $\langle A \rangle$. Meanwhile, we can also assume $-\mathbb{I}/2 \leq A \leq \mathbb{I}/2$

* ryuji.takagi@ntu.edu.sg

† suguru.endou.uc@hco.ntt.co.jp

‡ minagawa.shintaro@nagoya-u.jp

§ mgu@quantumcomplexity.org

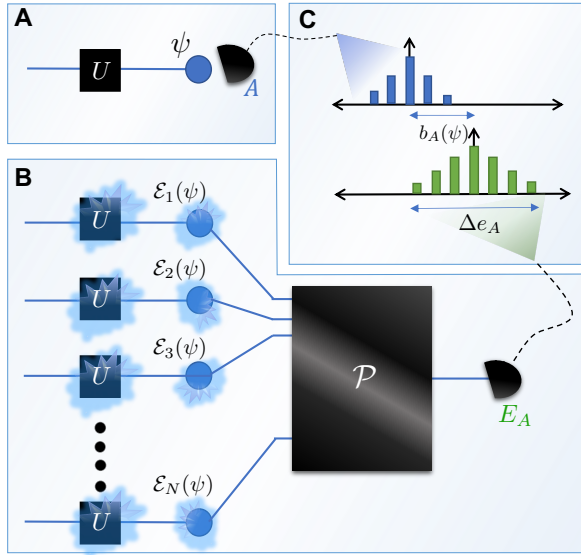


FIG. 1. General quantum error mitigation. (A) A major goal of many near-term algorithms is to estimate the expectation value of some observable A , when acting on the output ψ of some idealized computation U . (B) However, noise prevents exact synthesis of ψ . A general error-mitigation protocol attempts to estimate the true expectation value $\langle A \rangle = \text{Tr}(A\psi)$ by (1) using available NISQ devices to synthesize N distorted quantum states $\{\mathcal{E}_n(\psi)\}_{n=1}^N$ and (2) acting some physical process \mathcal{P} on these distorted states to produce a random variable E_A that approximates A . This procedure can then be repeated over M rounds to draw M samples of E_A , whose mean is used to estimate $\langle A \rangle$. (C) We can characterize the efficacy of such protocol by (1) its spread Δe_A , the difference between maximum and minimum possible of E_A and (2) the bias $b_A(\psi) = \langle E_A \rangle - \langle A \rangle$. Here we derive ultimate bounds on Δe_A for each given bias that no such error-mitigation protocol can exceed, as well as tighter bounds when \mathcal{P} is restricted only to coherent interactions over Q noisy devices at a time. This then tells us how many times \mathcal{P} must be executed to estimate $\langle A \rangle$ within some desired accuracy and failure probability.

without loss of generality. This is because any observable O can be shifted and rescaled to some A satisfying this condition, from which full information of O can be recovered [28]. Note also that while ψ is pure in many practically relevant instances, our analysis applies equally when ψ is mixed.

More formally, we introduce a framework encompassing any such error-mitigation protocol as follows. Each protocol begins by use of available NISQ devices to generate N distorted states $\mathcal{E}_1(\psi), \dots, \mathcal{E}_N(\psi)$, with effective noise channels $\{\mathcal{E}_n\}_{n=1}^N$ [29]. Here, \mathcal{E}_{n_1} is not necessarily equal to \mathcal{E}_{n_2} for $n_1 \neq n_2$, as general error-mitigation methods may involve noisy devices with tunable error (e.g., noise extrapolation [12, 13]). A *general error-mitigation strategy* can then be specified by some physical process \mathcal{P} that takes these distorted states as input and outputs some classical estimate random variable E_A of $\text{Tr}(A\psi)$ (See Fig. 1B). The aim is to generate E_A such that its expected value $\langle E_A \rangle$ is close to $\text{Tr}(A\psi)$. M rounds of this procedure then enables us to generate M samples of E_A , whose mean is used to estimate $\text{Tr}(A\psi)$.

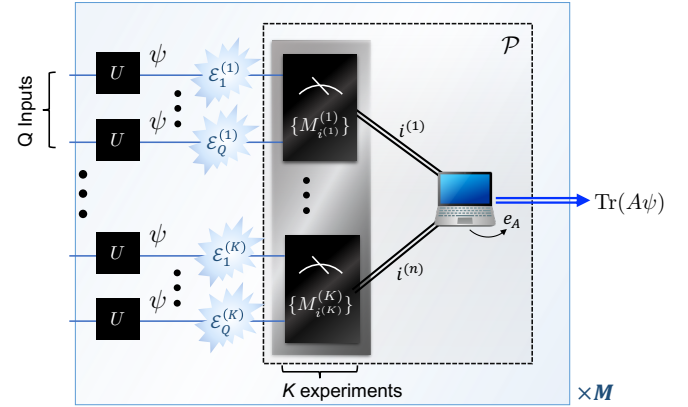


FIG. 2. Schematic of a (Q, K) -error mitigation protocol. A (Q, K) -error mitigation protocol is motivated when practical considerations limit the maximum number of distorted states that our mitigation process \mathcal{P} can coherently interact to Q . A general approach then divides these into $K = \lceil N/Q \rceil$ groups of size Q . To estimate $\langle A \rangle$ of some ideal output state ψ , each round of (Q, K) -mitigation involves first using available NISQ devices to generate Q copies of each distorted states $\mathcal{E}_q^{(k)}(\psi)$, for each of $k = 1, \dots, K$. These distorted states are then grouped together as inputs into K experiments, where each group consists of a single copy of each $\mathcal{E}_q^{(k)}(\psi)$. The k^{th} experiment then involves applying some general (possibly entangling) POVM $\{M_{i^{(k)}}^{(k)}\}$ on the k^{th} grouping, resulting in measurement outcome $i^{(k)}$. Classical computing is then deployed to produce an estimate $e_A(i^{(1)}, \dots, i^{(K)})$ whose average after M rounds of the above process is used to estimate $\text{Tr}(A\psi)$. Note that there can be additional quantum operations before the POVM measurements $\{M_{i^{(k)}}^{(k)}\}$, but these can be absorbed into the description of the POVMs without loss of generality.

Each choice of \mathcal{P} and N leads to a different error-mitigation strategy, and our performance bounds pertain to all possible choices of \mathcal{P} and N . However, we can often make these bounds tighter as practical limitations often constrain how many distorted states \mathcal{P} can coherently interact. Error mitigation protocols under such constraints typically select $N = KQ$ to a multiple of Q , such that the N distorted states are divided into K clusters, each containing Q distorted states. We label these as $\{\mathcal{E}_q^{(k)}(\psi)\}_{q=1, k=1}^{Q, K}$ for convenience. \mathcal{P} is then constrained to represent (i) local measurement procedures $M^{(k)}$ that can coherently interact distorted states within the k^{th} cluster (i.e., $\{\mathcal{E}_q^{(k)}(\psi)\}_{q=1}^Q$) to produce some classical interim outputs $i^{(k)}$ and (ii) classical post-processing e_A that transform the interim outputs $\{i^{(k)}\}_{k=1}^K$ into a sample of E_A .

We name such a protocol as *(Q, K) -error mitigation*, and refer to the generation of each $i^{(k)}$ as *an experiment*. Each round of a (Q, K) -error mitigation protocol thus contains K experiments on systems of up to Q distorted states [30]. We also summarize the above procedure in Fig. 2. This framework encompasses a broad class of error-mitigation strategies proposed so far [12, 13, 18, 21, 22, 31–35]. Fig. 3 and accompanying captions discuss how several prominent error-mitigation methods fit into this framework.

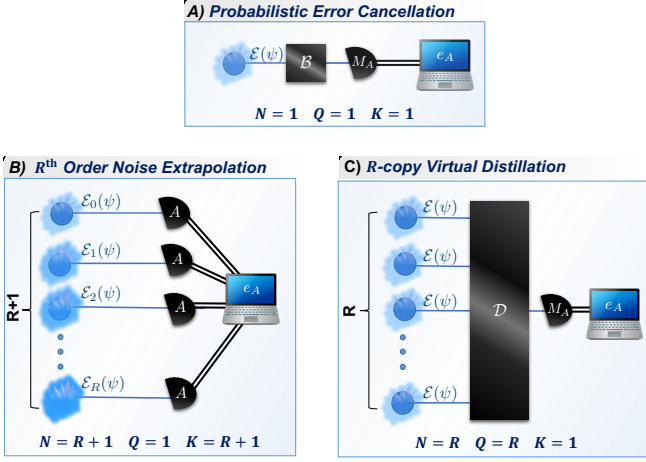


FIG. 3. Error-mitigation protocols. Our framework encompasses all commonly used error-mitigation protocols, a sample of which we outline here. (A) Probabilistic error cancellation [12] assumes we can only act a single coherent state each round, where it seeks to undo a given noise map \mathcal{E} by applying a suitable stochastic operation \mathcal{B} . Thus it corresponds to the case of $Q = K = 1$. (B) R^{th} order noise extrapolation assumes [12, 13] the capacity to synthesize $R + 1$ NISQ devices whose outputs represent distortions of ψ at various noise strengths. It then uses individual measurements of an observable A on these distorted states to estimate the observable expectation value on the zero-noise limit. Thus it is an example where $Q = 1$ and $K = R + 1$. (C) Meanwhile, R -copy virtual distillation [21, 22] involves running an available NISQ device R times to synthesize R copies of a distorted state $\mathcal{E}(\psi)$. Coherent interaction \mathcal{D} over these copies followed by a suitable measurement M_A then enables improved estimation of $\langle A \rangle$. Thus it is an example where $K = 1$ and $Q = R$. In Sec. IV and Appendix D, we provide a detailed account of each protocol and how it fits within our framework.

Quantifying performance — The performance of an error-mitigation protocol is determined by how well the random variable E_A governing each estimate aligns with $\text{Tr}(A\psi)$. We can characterize this by (i) its bias, representing how close $\langle E_A \rangle$ is to the ideal expectation value $\text{Tr}(A\psi)$ and (ii) its spread, representing the amount of intrinsic randomness within E_A .

A protocol’s bias quantifies the absolute minimum error to which it can estimate $\text{Tr}(A\psi)$, given no restrictions on many rounds it can run (i.e., samples of E_A it can draw). Mathematically, this is represented by the difference $b_A(\psi) = \langle E_A \rangle - \text{Tr}(A\psi)$. Since the error-mitigation strategy should work for arbitrary state ψ and observables A , we can introduce the *maximum bias*

$$b_{\max} := \max_{-1/2 \leq A \leq 1/2} \max_{\psi} [\langle E_A \rangle - \text{Tr}(A\psi)] \quad (1)$$

to bound the bias of an error-mitigation protocol at estimating expectation values over all output states and observables of interest. Hereafter, we will also assume $b_{\max} \leq 1/2$, as this condition must be satisfied for any meaningful error-mitigation protocol. This is because a maximum bias of $1/2$ can always be achieved by the trivial ‘error-mitigation’ protocol outputs $e_A = 0$ regardless of ψ or A .

Of course, having $b_{\max} = 0$ still does not guarantee an effective error-mitigation protocol. Each sample of E_A will also deviate from $\text{Tr}(A\psi)$ due to intrinsic random error. The greater this randomness, the more samples we need from E_A to ensure that the mean of our samples is a reliable estimate of its true expectation value $\langle E_A \rangle$. The relation is formalized by Hoeffding’s inequality [36]. Namely, suppose $\{x_i\}_{i=1}^M$ are M samples of a random variable X with $x_i \in [a, b]$, the number of samples M required to ensure an estimation error $|\langle X \rangle - \sum_i x_i/M| < \delta$ with probability $1 - \varepsilon$ is given by $\frac{2(a-b)^2}{\delta^2} \log(2/\varepsilon)$. This means that to ensure a desired accuracy and reliability, one needs the number of samples proportional to the square of range $|a - b|$ of the random variable X . In our context, this corresponds to the *maximum spread* in the outcomes of estimator function e_A defined by

$$\Delta e_{\max} := \max_{-1/2 \leq A \leq 1/2} \Delta e_A, \quad (2)$$

where Δe_A is the difference between the maximum and minimum possible values of E_A can take [37].

Δe_{\max} thus directly relates to the sampling cost of an error-mitigation protocol. Given an error-mitigation protocol whose estimates have maximum spread Δe_{\max} , we know that it must at least sample E_A of order $\Omega(\Delta e_{\max}^2 \log(1/\varepsilon)/\delta^2)$ times to ensure that its estimate of $\langle E_A \rangle$ has accuracy δ and failure rate ε . Therefore, we may think of Δe_{\max} as a measure of computational cost or feasibility. Its exponential scaling with respect to the circuit depth, for example, would imply eventual intractability in mitigating associated errors in a class of non-shallow circuits.

III. FUNDAMENTAL LIMITS

Our main contribution is to establish a universal lower bound on Δe_{\max} that assumes only the laws of quantum mechanics. Our bound then determines the number of times an error-mitigation method needs to sample E_A (and thus the number of times we must invoke a NISQ device) to estimate A within some tolerable error.

To state the bound formally, we utilize measures of state distinguishability. Consider the scenario where Alice prepares a quantum state in either ρ and σ and challenges Bob to guess which is prepared. The trace distance $D_{\text{tr}}(\rho, \sigma) = \frac{1}{2} \|\rho - \sigma\|_1$ (where $\|\cdot\|_1$ is the trace norm) then represents the quantity such that Bob’s optimal probability of guessing correctly is $\frac{1}{2}(1 + D_{\text{tr}}(\rho, \sigma))$. When ρ and σ describe states on K -partite systems $S_1 \otimes \dots \otimes S_K$, we can also consider the setting in which Bob is constrained to local measurements, resulting in the optimal guessing probability $\frac{1}{2}(1 + D_{\text{LM}}(\rho, \sigma))$ where D_{LM} is the local distinguishability measure [38] (see also Appendix B). In our setting, we identify each local subsystem S_k with a system corresponding to the k^{th} experiment in Fig. 2. We are then in a position to state our main result:

Theorem 1. Consider an arbitrary (Q, K) -mitigation protocol with maximum bias b_{\max} . Then, its maximum spread Δe_{\max} is

lower bounded by

$$\Delta e_{\max} \geq \max_{\psi, \phi} \frac{D_{\text{tr}}(\psi, \phi) - 2b_{\max}}{D_{\text{LM}}(\mathcal{L}(\psi), \mathcal{L}(\phi))} \quad (3)$$

where $\mathcal{L}(\cdot) := \otimes_{k=1}^K \otimes_{q=1}^Q \mathcal{E}_q^{(k)}(\cdot)$, and $\mathcal{E}_q^{(k)}$ describes its effective noise channel for the q^{th} input in the k^{th} experiment.

Combining this with Hoeffding's inequality immediately leads to the following bound on the sampling cost.

Corollary 2. Consider an arbitrary (Q, K) -mitigation protocol with maximum bias b_{\max} . The number of samples M required to guarantee an estimation error of at most $b_{\max} + \delta$ with probability $1 - \epsilon$ satisfies

$$M \geq \left[\max_{\psi, \phi} \frac{D_{\text{tr}}(\psi, \phi) - 2b_{\max}}{D_{\text{LM}}(\mathcal{L}(\psi), \mathcal{L}(\phi))} \right]^2 \frac{2 \log(2/\epsilon)}{\delta^2} \quad (4)$$

where $\mathcal{L}(\cdot) := \otimes_{k=1}^K \otimes_{q=1}^Q \mathcal{E}_q^{(k)}(\cdot)$.

Theorem 1 and Corollary 2 offer two immediate qualitative insights. The first is the potential trade-off between sampling cost and systematic error — we may reduce the sampling cost by increasing tolerance for bias. The second is a direct relation between sampling cost and distinguishability — the more a noise source degrades distinguishability between states, the more costly the error is to mitigate.

The intuition behind this relation rests on the observation that the error-mitigation process is a quantum channel. Thus, any error-mitigation procedure must obey data-processing inequalities for distinguishability (see Appendix A). On the other hand, error mitigation aims to improve our ability to estimate expectation values of various observables, which would enhance our ability to distinguish between noisy states. The combination of these observations then implies that distinguishability places a fundamental constraint on required sampling costs to mitigate error. For details of the associated proof, see Appendix B.

We note also that our bound involves the local distinguishability $D_{\text{LM}}(\rho, \sigma)$ rather than the standard trace distance $D_{\text{tr}}(\rho, \sigma)$. This is due to the constraints we placed of \mathcal{P} that limits it to coherently interacting the outputs of a finite number of NISQ devices — reflecting the hybrid nature of quantum error mitigation utilizing quantum and classical resources in tandem. Indeed, since $D_{\text{tr}}(\rho, \sigma) \geq D_{\text{LM}}(\rho, \sigma)$ (as constraining measurements to be local cannot ever improve distinguishability), our theorem also implies

$$\Delta e_{\max} \geq \max_{\psi, \phi} \frac{D_{\text{tr}}(\psi, \phi) - 2b_{\max}}{D_{\text{tr}}(\mathcal{L}(\psi), \mathcal{L}(\phi))} \quad (5)$$

as an immediate corollary, giving another lower bound on the sampling cost as in Corollary 2. This bound represents the ultimate performance limits of all (Q, K) error-mitigation protocols that coherently operate on $N = QK$ distorted states each round.

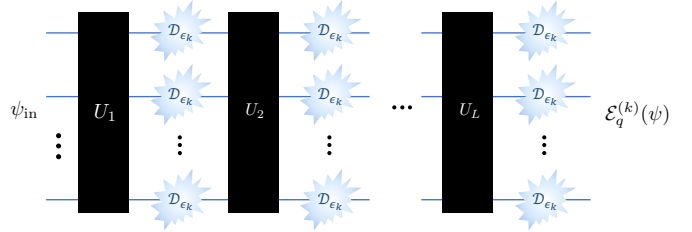


FIG. 4. Noise mitigation in layered circuits. Layered circuits are used extensively in variational algorithms for NISQ devices. They involve repeated layers of gates, each consisting of some unitary U_l . A standard noise model for such circuits involves the action of local depolarizing noise \mathcal{D}_ϵ on each qubit during each layer of the circuit. The k^{th} experiment in a general (Q, K) -protocol involves running this circuit Q times to produce a distorted state $\otimes_{q=1}^Q \mathcal{E}_q^{(k)}(\psi)$ with some noise strength ϵ_k — which possibly varies over different experiments. The protocol then measures each $\otimes_{q=1}^Q \mathcal{E}_q^{(k)}(\psi)$ for $k = 1, \dots, K$ and outputs an estimate E_A through classical post-processing of the measurements results.

IV. APPLICATIONS

Quantitatively, the above bounds enable us to determine the ultimate performance limits of error mitigation given a particular set of imperfect quantum devices specified by error channels $\{\mathcal{E}_q^{(k)}\}$. In the subsequent section, we illustrate how this (i) enables the identification of unavoidable sampling overheads when performing error mitigation on a common class of NISQ algorithms, and (ii) provides a means to benchmark existing error-mitigation protocols to identify if there is potential room for improvement.

Error-mitigating layered circuits — Our first application is to identify the ultimate sampling overhead required to mitigate errors on a class of layered circuits used extensively in variational quantum eigensolvers [39]. Variational algorithms typically assume a quantum circuit consisting of multiple layers of unitary gates $\{U_l\}_{l=1}^L$. Indeed, as designed with NISQ applications in mind, they are a key candidate for benchmarking of error-mitigation protocols [16, 40, 41].

In particular, consider a local depolarizing noise [27, 42], in which the depolarizing channel $\mathcal{D}_\epsilon(\rho) := (1 - \epsilon)\rho + \epsilon\mathbb{I}/2$ acts on each qubit. A general approach to mitigate this error is to employ an (Q, K) -mitigation protocol for some Q and K , in which the k^{th} experiment involves depolarizing noise with noise strength ϵ_k (Fig. 4).

Taking $U = U_L \cdots U_2 U_1$ in Fig. 2 and applying Theorem 1 to this setting, we obtain the following bound (See Appendix C for the proof).

Theorem 3. For an arbitrary (Q, K) -error mitigation with maximum bias b_{\max} applied to L -layer circuits under local depolarizing noise, the maximum spread is lower bounded as

$$\Delta e_{\max} \geq \frac{1 - 2b_{\max}}{\sqrt{2 \ln 2} \sqrt{NQ} K} \left(\frac{1}{1 - \epsilon_{\min}} \right)^{L/2}, \quad (6)$$

where $\epsilon_{\min} := \min_k \epsilon_k$ is the minimum noise strength among K experiments.

Theorem 3 implies that exponentially many samples with respect to the circuit depth L are required for arbitrary error-mitigation strategies encompassed in our framework. This formally validates our intuition that information should quickly get degraded due to the sequential noise effects, incurring exponential overhead to remove the accumulated noise effect.

Protocol benchmarking—Theorems 1 and 3 place strategy-independent bounds on sampling cost for each Q and K and available noise channels $\mathcal{E}_q^{(k)}$, enabling us to identify the ultimate potential of error mitigation under various noise settings and operational constraints. Comparing this limit with that achieved by specific known methods of error mitigation then provides a valuable benchmark, helping us assess their optimality and quantify the potential room for improvement. We illustrate this here by considering probabilistic error cancellation [12], and provide detailed analysis of other prominent error-mitigation protocols in Appendix D.

Probabilistic error cancellation is an error-mitigation protocol that produces an unbiased estimate of $\text{Tr}(A\psi)$ using a distorted state $\mathcal{E}(\psi)$ each round (see Fig 3A). As such, it fulfills the criteria of being a $(1, 1)$ -protocol, i.e., $Q = K = 1$, with $b_{\max} = 0$. Specifically, probabilistic error cancellation operates by identifying a complete basis of processes $\{\mathcal{B}_j\}_j$ such that $\mathcal{E}^{-1} = \sum_j c_j \mathcal{B}_j$ for some set of real (but possibly negative) numbers $\{c_j\}_j$. Setting $\gamma := \sum_j |c_j|$, the protocol then (a) applies \mathcal{B}_j to the noisy state $\mathcal{E}(\psi)$ with probability $p_j = |c_j|/\gamma$, (b) measures A to get outcome a_j , and (c) multiplies each outcome by $\gamma \text{sgn}(c_j)$ and takes the average.

In the context of our framework, we can introduce a quantum operation \mathcal{B} that represents first initializing a classical register to a state j with probability p_j and applying \mathcal{B}_j to $\mathcal{E}(\psi)$ conditioned on j . Meanwhile, M_A represents an A -measurement of the resulting quantum system combined with a measurement of the register, resulting in the outcome pair (a_j, j) . Taking $e_A^{\text{PEC}}((a_j, j)) = \gamma \text{sgn}(c_j) a_j$, we see that the maximum spread of this estimator is given by

$$\Delta e_{\max}^{\text{PEC}} = \gamma, \quad (7)$$

a well-studied quantity that is already associated with the sampling overhead of probabilistic error cancellation [12].

The optimal sampling cost γ_{opt} is then achieved by minimizing such γ over all feasible $\{\mathcal{B}_j\}_j$ [43]. Once computed for a specific noise channel \mathcal{E} , we can compare it to fundamental lower bounds in Theorem 1 to determine if there is possible room for improvement.

In the case of qubit dephasing $\mathcal{Z}_\epsilon(\rho) := (1 - \epsilon)\rho + \epsilon Z\rho Z$, the optimal cost was obtained as [43–45]

$$\gamma_{\text{opt}} = \Delta e_{\max}^{\text{PEC}} = \frac{1}{1 - 2\epsilon}. \quad (8)$$

This can be compared to the bound for Δe_{\max} from Theorem 1 that applies to every mitigation protocol with $Q = K = 1$. Note

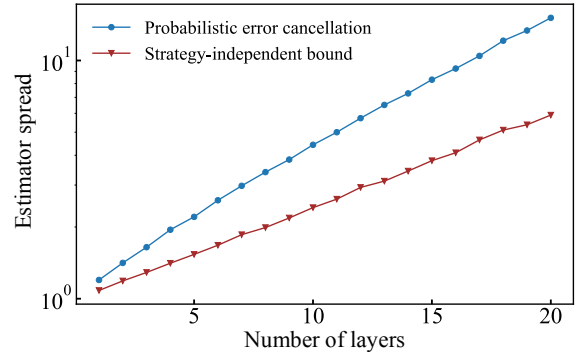


FIG. 5. **Performance of probabilistic error cancellation for a layered circuit.** The strategy-independent lower bound for $Q = K = 1$ (brown triangles) and the spread for probabilistic error cancellation (blue dots). Each data point of the strategy-independent bound was obtained by evaluating 10^2 pairs of output states from a noisy hardware-efficient ansatz circuit and taking the maximum value that gives the tightest bound.

that, since $K = 1$, $D_{\text{LM}} = D_{\text{tr}}$. By a direct calculation, we get

$$\max_{\psi, \phi} \frac{D_{\text{tr}}(\psi, \phi)}{D_{\text{tr}}(\mathcal{Z}_\epsilon(\psi), \mathcal{Z}_\epsilon(\phi))} \geq \frac{D_{\text{tr}}(|+\rangle\langle +|, |-\rangle\langle -|)}{D_{\text{tr}}(\mathcal{Z}_\epsilon(|+\rangle\langle +|), \mathcal{Z}_\epsilon(|-\rangle\langle -|))} = \frac{1}{1 - 2\epsilon} \quad (9)$$

where $|\pm\rangle := (|0\rangle \pm |1\rangle)/\sqrt{2}$. Remarkably, the two quantities—the maximum spread for the probabilistic error cancellation and the lower bound for arbitrary unbiased mitigation strategies with $Q = K = 1$ —exactly coincide. This shows that the probabilistic error cancellation achieves the ultimate performance limit of unbiased $(1, 1)$ -protocols for correcting qubit-dephasing noise.

Let us also consider the d -dimensional depolarizing noise $\mathcal{D}_\epsilon^d(\rho) = (1 - \epsilon)\rho + \epsilon \mathbb{I}/d$. The optimal overhead cost for this noise was obtained as [43–45]

$$\gamma_{\text{opt}} = \Delta e_{\max}^{\text{PEC}} = \frac{1 + (1 - 2/d^2)\epsilon}{1 - \epsilon}. \quad (10)$$

This can be compared to the bound from Theorem 1

$$\max_{\psi, \phi} \frac{D_{\text{tr}}(\psi, \phi)}{D_{\text{tr}}(\mathcal{D}_\epsilon^d(\psi), \mathcal{D}_\epsilon^d(\phi))} = \frac{1}{1 - \epsilon}, \quad (11)$$

which is slightly lower than $\Delta e_{\max}^{\text{PEC}}$ in (10), with difference being $O(\epsilon)$. This suggests that probabilistic error cancellation is nearly optimal for this noise model, while still leaving possibility for a better protocol to exist.

For completeness, we can also revisit the case of layered circuits (i.e., take $U = U_L \cdots U_2 U_1$ in Fig. 2). In this context, we can determine the ultimate achievable spread $\Delta e_{\max}^{\text{PEC}}$ by choosing $\{\mathcal{B}_j\}_j$ as the set of all quantum operations [46]. In Fig. 5, we compare this against our strategy-independent lower bound (see Appendix E for details). We see that our general lower bound indeed places an ultimate limit on $\Delta e_{\max}^{\text{PEC}}$, which scales exponentially with the number of layers as suggested by Theorem 3.

V. CONCLUSIONS

We introduced a general framework for quantum error mitigation that considers estimating the expected measurement outcomes of ideal quantum circuits by performing measurements on noisy circuits. We employed this framework to derive universal performance bounds — implied by the laws of quantum mechanics — that determine how many extra repetitions an error-mitigation protocol requires to ensure estimates to fall within a given accuracy range with some guaranteed probability of success. Our bounds have immediate consequences. For layered circuits under the local depolarizing noise, they imply that the sampling overhead for error mitigation must scale exponentially with respect to the circuit depth. Meanwhile, we illustrated that probabilistic error cancellation can saturate such bounds for a certain noise model, implying its provable optimality. More generally, our bounds provide a means of identifying when current state-of-the-art error mitigation methods have the greatest room for improvement.

We note that our performance bounds have focused on the scaling of M , representing how many rounds an error-mitigation protocol must be run to get a reliable estimate of some observable $\langle A \rangle$. Although this analysis is sufficient for many present methods of error mitigation, it is possible to also improve estimates of $\langle A \rangle$ by scaling the number of distorted outputs we process in a single round (e.g., subspace expansion [31] and exponential extrapolation [18]). While our framework in Fig. 1 encompasses such methodologies — and as such all bounds on estimation error apply — full understanding of the performance of such protocols would involve further investigation on how estimation error scales with respect to N or K . This then presents a natural direction for future research.

Our results also offer potential insights into several related fields. Non-Markovian dynamics have shown promise in decreasing sampling costs in error mitigation [47]. Since non-Markovianity is known to be deeply related to the trace distance [48], our newly established relations between trace distance and quantum error mitigation hint at promising relations between the two fields. The second direction is to relate our general framework of quantum error mitigation to the established theory of quantum error correction. Quantum error

correction concerns algorithms that prevent degrading trace distance between suitably encoded logical states, while our results indicate that less reduction in trace distance can enable smaller error mitigation costs. Thus, our work provides a toolkit for identifying fundamental bounds in the transition from error mitigation to error correction as we proceed from NISQ devices towards scalable quantum computing. This then complements presently active research in error suppression that combines the two techniques [49–52]. Beyond error suppression, quantum protocols in many diverse settings also share the structure of classical post-processing of quantum measurements — from quantum metrology and illumination to hypothesis testing and stochastic analysis [53–57]. Our framework — suitably extended — could thus identify new performance bounds in each of these settings.

Note added.—During the completion of our manuscript, we became aware of an independent work by Wang *et al.* [58], which showed a result related to our Theorem 3 on the exponential scaling of required samples in variational algorithms.

ACKNOWLEDGMENTS

We thank Yuichiro Matsuzaki, Yuuki Tokunaga, Hideaki Hakoshima, Kaoru Yamamoto, and Francesco Buscemi for fruitful discussions. This research is supported by the Singapore Ministry of Education Tier 1 Grant RG162/19, the NRF-ANR joint program (NRF2017-NRF-ANR004 VanQuTe), the Quantum Engineering Program QEP-SF3, the National Research Foundation (NRF) Singapore, under its NRFF Fellow program (Award No. NRF-NRFF2016-02), FQXi-RFP-IPW-1903 project from the Foundational Questions Institute and Fetzer Franklin Fund, a donor advised fund of Silicon Valley Community Foundation. Any opinions, findings and conclusions or recommendations expressed in this material are those of the author(s) and do not reflect the views of National Research Foundation or the Ministry of Education, Singapore. S.E. is supported by ERATO, JST, Grant No. JPMJER1601; Moonshot R&D, JST, Grant No. JPMJMS2061; MEXT Q-LEAP Grant No. JPMXS0120319794 and JPMXS0118068682. Numerical simulations have been performed with QuTiP [59].

[1] J. Preskill, *Quantum Computing in the NISQ era and beyond*, *Quantum* **2**, 79 (2018).

[2] F. Arute *et al.*, *Quantum supremacy using a programmable superconducting processor*, *Nature* **574**, 505 (2019).

[3] A. G. Fowler, M. Mariantoni, J. M. Martinis, and A. N. Cleland, *Surface codes: Towards practical large-scale quantum computation*, *Phys. Rev. A* **86**, 032324 (2012).

[4] E. T. Campbell, B. M. Terhal, and C. Vuillot, *Roads towards Fault-Tolerant Universal Quantum Computation*, *Nature* **549**, 172 (2017).

[5] S. McArdle, S. Endo, A. Aspuru-Guzik, S. C. Benjamin, and X. Yuan, *Quantum computational chemistry*, *Rev. Mod. Phys.* **92**, 015003 (2020).

[6] S. Endo, Z. Cai, S. C. Benjamin, and X. Yuan, *Hybrid Quantum-Classical Algorithms and Quantum Error Mitigation*, *J. Phys. Soc. Jpn.* **90**, 032001 (2021).

[7] M. Cerezo, A. Arrasmith, R. Babbush, S. C. Benjamin, S. Endo, K. Fujii, J. R. McClean, K. Mitarai, X. Yuan, L. Cincio, *et al.*, *Variational quantum algorithms*, *Nat. Rev. Phys.* , 1 (2021).

[8] K. Bharti, A. Cervera-Lierta, T. H. Kyaw, T. Haug, S. Alperin-Lea, A. Anand, M. Degroote, H. Heimonen, J. S. Kottmann, T. Menke, *et al.*, *Noisy intermediate-scale quantum (NISQ) algorithms*, (2021), [arXiv:2101.08448](https://arxiv.org/abs/2101.08448).

[9] A. Kandala, A. Mezzacapo, K. Temme, M. Takita, M. Brink, J. M. Chow, and J. M. Gambetta, *Hardware-efficient variational quantum eigensolver for small molecules and quantum magnets*,

Nature **549**, 242 (2017).

[10] Y. Cao, J. Romero, J. P. Olson, M. Degroote, P. D. Johnson, M. Kieferová, I. D. Kivlichan, T. Menke, B. Peropadre, N. P. Sawaya, *et al.*, *Quantum chemistry in the age of quantum computing*, *Chem. Rev.* **119**, 10856 (2019).

[11] S. McArdle, X. Yuan, and S. Benjamin, *Error-Mitigated Digital Quantum Simulation*, *Phys. Rev. Lett.* **122**, 180501 (2019).

[12] K. Temme, S. Bravyi, and J. M. Gambetta, *Error Mitigation for Short-Depth Quantum Circuits*, *Phys. Rev. Lett.* **119**, 180509 (2017).

[13] Y. Li and S. C. Benjamin, *Efficient Variational Quantum Simulator Incorporating Active Error Minimization*, *Phys. Rev. X* **7**, 021050 (2017).

[14] T. Giurgica-Tiron, Y. Hindy, R. LaRose, A. Mari, and W. J. Zeng, *Digital zero noise extrapolation for quantum error mitigation*, *2020 IEEE International Conference on Quantum Computing and Engineering (QCE)*, 306 (2020).

[15] A. He, B. Nachman, W. A. de Jong, and C. W. Bauer, *Zero-noise extrapolation for quantum-gate error mitigation with identity insertions*, *Phys. Rev. A* **102**, 012426 (2020).

[16] A. Kandala, K. Temme, A. D. Córcoles, A. Mezzacapo, J. M. Chow, and J. M. Gambetta, *Error mitigation extends the computational reach of a noisy quantum processor*, *Nature* **567**, 491 (2019).

[17] E. F. Dumitrescu, A. J. McCaskey, G. Hagen, G. R. Jansen, T. D. Morris, T. Papenbrock, R. C. Pooser, D. J. Dean, and P. Lougovski, *Cloud Quantum Computing of an Atomic Nucleus*, *Phys. Rev. Lett.* **120**, 210501 (2018).

[18] S. Endo, S. C. Benjamin, and Y. Li, *Practical Quantum Error Mitigation for Near-Future Applications*, *Phys. Rev. X* **8**, 031027 (2018).

[19] C. Song, J. Cui, H. Wang, J. Hao, H. Feng, and Y. Li, *Quantum computation with universal error mitigation on a superconducting quantum processor*, *Sci. Adv.* **5**, eaaw5686 (2019).

[20] S. Zhang, Y. Lu, K. Zhang, W. Chen, Y. Li, J.-N. Zhang, and K. Kim, *Error-mitigated quantum gates exceeding physical fidelities in a trapped-ion system*, *Nat. Commun.* **11**, 587 (2020).

[21] B. Koczor, *Exponential Error Suppression for Near-Term Quantum Devices*, *Phys. Rev. X* **11**, 031057 (2021).

[22] W. J. Huggins, S. McArdle, T. E. O'Brien, J. Lee, N. C. Rubin, S. Boixo, K. B. Whaley, R. Babbush, and J. R. McClean, *Virtual Distillation for Quantum Error Mitigation*, (2020), [arXiv:2011.07064](https://arxiv.org/abs/2011.07064).

[23] P. Czarnik, A. Arrasmith, L. Cincio, and P. J. Coles, *Qubit-efficient exponential suppression of errors*, (2021), [arXiv:2102.06056](https://arxiv.org/abs/2102.06056).

[24] Z. Cai, *Resource-efficient Purification-based Quantum Error Mitigation*, (2021), [arXiv:2107.07279](https://arxiv.org/abs/2107.07279).

[25] M. Huo and Y. Li, *Dual-state purification for practical quantum error mitigation*, (2021), [arXiv:2105.01239](https://arxiv.org/abs/2105.01239).

[26] Y. Xiong, S. X. Ng, and L. Hanzo, *Quantum error mitigation relying on permutation filtering*, (2021), [arXiv:2107.01458](https://arxiv.org/abs/2107.01458).

[27] S. Wang, E. Fontana, M. Cerezo, K. Sharma, A. Sone, L. Cincio, and P. J. Coles, *Noise-Induced Barren Plateaus in Variational Quantum Algorithms*, (2020), [arXiv:2007.14384](https://arxiv.org/abs/2007.14384).

[28] For instance, if we are interested in a non-identity Pauli operator P , which has eigenvalues ± 1 , we instead consider an observable $A = P/2$.

[29] The effective noise channel is a map that connects an ideal state to a distorted state and may be different from the actual noise channel that happens in the NISQ device. Nevertheless, one can always find such an effective noise channel given the descriptions of the actual noise channels and the idealized circuit U .

[30] In principle, one can consider a different number of inputs Q_k for each k^{th} experiment, which may find a better fit to a recent proposal [34]. Such scenarios are still encompassed in the present framework by setting $Q = \max_k Q_k$, but it may result in a tighter bound in Theorem 1.

[31] J. R. McClean, M. E. Kimchi-Schwartz, J. Carter, and W. A. de Jong, *Hybrid quantum-classical hierarchy for mitigation of decoherence and determination of excited states*, *Phys. Rev. A* **95**, 042308 (2017).

[32] X. Bonet-Monroig, R. Sagastizabal, M. Singh, and T. E. O'Brien, *Low-cost error mitigation by symmetry verification*, *Phys. Rev. A* **98**, 062339 (2018).

[33] S. Bravyi, S. Sheldon, A. Kandala, D. C. McKay, and J. M. Gambetta, *Mitigating measurement errors in multiqubit experiments*, *Phys. Rev. A* **103**, 042605 (2021).

[34] N. Yoshioka, H. Hakoshima, Y. Matsuzaki, Y. Tokunaga, Y. Suzuki, and S. Endo, *Generalized quantum subspace expansion*, (2021), [arXiv:2107.02611](https://arxiv.org/abs/2107.02611).

[35] J. R. McClean, Z. Jiang, N. C. Rubin, R. Babbush, and H. Neven, *Decoding quantum errors with subspace expansions*, *Nat. Commun.* **11**, 636 (2020).

[36] W. Hoeffding, *Probability Inequalities for Sums of Bounded Random Variables*, *J. Am. Stat. Assoc.* **58**, 13 (1963).

[37] Mathematically, $\Delta e_A = e_{A,\max} - e_{A,\min}$ where $\Delta e_{A,\max} = \max_{i^{(1)} \dots i^{(K)}} e_A(i^{(1)} \dots i^{(K)})$ and $e_{A,\min} = \min_{i^{(1)} \dots i^{(K)}} e_A(i^{(1)} \dots i^{(K)})$.

[38] W. Matthews, S. Wehner, and A. Winter, *Distinguishability of Quantum States Under Restricted Families of Measurements with an Application to Quantum Data Hiding*, *Commun. Math. Phys.* **291**, 813 (2009).

[39] A. Peruzzo, J. McClean, P. Shadbolt, M.-H. Yung, X.-Q. Zhou, P. J. Love, A. Aspuru-Guzik, and J. L. O'Brien, *A variational eigenvalue solver on a photonic quantum processor*, *Nat. Commun.* **5**, 4213 (2014).

[40] Y. Kim, C. J. Wood, T. J. Yoder, S. T. Merkel, J. M. Gambetta, K. Temme, and A. Kandala, *Scalable error mitigation for noisy quantum circuits produces competitive expectation values*, (2021), [arXiv:2108.09197](https://arxiv.org/abs/2108.09197).

[41] R. Sagastizabal, X. Bonet-Monroig, M. Singh, M. A. Rol, C. C. Bultink, X. Fu, C. H. Price, V. P. Ostroukh, N. Muthusubramanian, A. Bruno, M. Beekman, N. Haider, T. E. O'Brien, and L. DiCarlo, *Experimental error mitigation via symmetry verification in a variational quantum eigensolver*, *Phys. Rev. A* **100**, 010302 (2019).

[42] A. Müller-Hermes, D. Stilck França, and M. M. Wolf, *Relative entropy convergence for depolarizing channels*, *J. Math. Phys.* **57**, 022202 (2016).

[43] R. Takagi, *Optimal resource cost for error mitigation*, *Phys. Rev. Research* **3**, 033178 (2021).

[44] J. Jiang, K. Wang, and X. Wang, *Physical Implementability of Quantum Maps and Its Application in Error Mitigation*, [arXiv:2012.10959](https://arxiv.org/abs/2012.10959).

[45] B. Regula, R. Takagi, and M. Gu, *Operational applications of the diamond norm and related measures in quantifying the non-physicality of quantum maps*, *Quantum* **5**, 522 (2021).

[46] In this case, the spread γ_{opt} coincides with the diamond norm of the inverse of the effective noise channel [45].

[47] H. Hakoshima, Y. Matsuzaki, and S. Endo, *Relationship between costs for quantum error mitigation and non-Markovian measures*, *Phys. Rev. A* **103**, 012611 (2021).

[48] H.-P. Breuer, E.-M. Laine, J. Piilo, and B. Vacchini, *Colloquium: Open quantum systems*, *Rev. Mod. Phys.* **82**, 287 (2010).

Non-Markovian dynamics in open quantum systems, *Rev. Mod. Phys.* **88**, 021002 (2016).

[49] Y. Suzuki, S. Endo, K. Fujii, and Y. Tokunaga, *Quantum error mitigation for fault-tolerant quantum computing*, (2020), [arXiv:2010.03887](https://arxiv.org/abs/2010.03887).

[50] M. Lostaglio and A. Ciani, *Error mitigation and quantum-assisted simulation in the error corrected regime*, (2021), [arXiv:2103.07526](https://arxiv.org/abs/2103.07526).

[51] C. Piveteau, D. Sutter, S. Bravyi, J. M. Gambetta, and K. Temme, *Error mitigation for universal gates on encoded qubits*, (2021), [arXiv:2103.04915](https://arxiv.org/abs/2103.04915).

[52] Y. Xiong, D. Chandra, S. X. Ng, and L. Hanzo, *Sampling Overhead Analysis of Quantum Error Mitigation: Uncoded vs. Coded Systems*, *IEEE Access* **8**, 228967 (2020).

[53] S. Lloyd, *Enhanced sensitivity of photodetection via quantum illumination*, *Science* **321**, 1463 (2008).

[54] V. Giovannetti, S. Lloyd, and L. Maccone, *Quantum Metrology*, *Phys. Rev. Lett.* **96**, 010401 (2006).

[55] K. M. Audenaert, M. Nussbaum, A. Szkoła, and F. Verstraete, *Asymptotic error rates in quantum hypothesis testing*, *Commun. Math. Phys.* **279**, 251 (2008).

[56] F. C. Binder, J. Thompson, and M. Gu, *Practical Unitary Simulator for Non-Markovian Complex Processes*, *Phys. Rev. Lett.* **120**, 240502 (2018).

[57] C. Blank, D. K. Park, and F. Petruccione, *Quantum-enhanced analysis of discrete stochastic processes*, *npj Quantum Inf.* **7**, 1–9 (2021).

[58] S. Wang, P. Czarnik, A. Arrasmith, M. Cerezo, L. Cincio, and P. J. Coles, *Can Error Mitigation Improve Trainability of Noisy Variational Quantum Algorithms?*, (2021), [arXiv:2109.01051](https://arxiv.org/abs/2109.01051).

[59] J. R. Johansson, P. D. Nation, and F. Nori, *QuTiP: An open-source Python framework for the dynamics of open quantum systems*, *Comput. Phys. Commun.* **183**, 1760 (2012).

[60] L. Lami, C. Palazuelos, and A. Winter, *Ultimate Data Hiding in Quantum Mechanics and Beyond*, *Commun. Math. Phys.* **361**, 661 (2018).

[61] W. H. G. Corrêa, L. Lami, and C. Palazuelos, *Maximal gap between local and global distinguishability of bipartite quantum states*, (2021), [arXiv:2110.04387](https://arxiv.org/abs/2110.04387).

[62] F. Hiai, M. Ohya, and M. Tsukada, *Sufficiency, KMS condition and relative entropy in von Neumann algebras.*, *Pac. J. Math.* **96**, 99 (1981).

[63] The bias for Richardson extrapolation in (D2) is represented by a polynomial with respect to the base noise strength ξ . In the layered circuit, this is roughly the noise strength of the total effective noise channel, which grows with the number of layers due to the noise accumulation.

[64] B. Koczor, *The Dominant Eigenvector of a Noisy Quantum State*, (2021), [arXiv:2104.00608](https://arxiv.org/abs/2104.00608).

[65] Z. Cai, *Multi-exponential error extrapolation and combining error mitigation techniques for NISQ applications*, *npj Quantum Inf.* **7**, 80 (2021).

[66] J. Sun, X. Yuan, T. Tsunoda, V. Vedral, S. C. Benjamin, and S. Endo, *Mitigating Realistic Noise in Practical Noisy Intermediate-Scale Quantum Devices*, *Phys. Rev. Applied* **15**, 034026 (2021).

[67] A. Mari, N. Shammah, and W. J. Zeng, *Extending quantum probabilistic error cancellation by noise scaling*, (2021), [arXiv:2108.02237](https://arxiv.org/abs/2108.02237).

Appendix A: Error mitigation and distinguishability

The goal of quantum error mitigation is to estimate the expectation value of an arbitrary observable A for an arbitrary ideal state ψ only using the noisy state $\mathcal{E}(\psi)$. Although $\text{Tr}(A\mathcal{E}(\psi))$ can deviate from $\text{Tr}(A\psi)$, error mitigation correctly allows us to estimate $\text{Tr}(A\psi)$, which appears to have eliminated noise effects. Since each error-mitigation strategy should also work for another state ϕ , it should be able to remove the noise and estimate $\text{Tr}(A\phi)$ out of $\text{Tr}(A\mathcal{E}(\phi))$. Does this ‘removal’ of noise imply that error mitigation can help distinguish $\mathcal{E}(\psi)$ and $\mathcal{E}(\phi)$?

The subtlety of this question can be seen by looking at how quantum error mitigation works. The estimation of $\text{Tr}(A\mathcal{E}(\psi))$ without error mitigation is carried out by making a measurement with respect to the eigenbasis of $A = \sum_a a|a\rangle\langle a|$, which produces a probability distribution $p(a|\mathcal{E}(\psi), A)$ over possible outcomes $\{a\}$. Because of the noise, the expectation value of this distribution is shifted from $\text{Tr}(A\psi)$. Similarly, the same measurement for a state $\mathcal{E}(\phi)$ produces a probability distribution $p(a|\mathcal{E}(\phi), A)$, whose expectation value may also be shifted from $\text{Tr}(A\phi)$. Error-mitigation protocol applies additional operations, measurements and classical post-processing to produce other probability distributions $p_{\text{EM}}(a|\mathcal{E}(\psi), A)$ and $p_{\text{EM}}(a|\mathcal{E}(\phi), A)$ whose expectation values get closer to the original ones. As a result, although the expectation values of the two error-mitigated distributions get separated from each other, they also get broader, which may increase the overlap between the two distributions, possibly making it even harder to distinguish two distributions. (See Fig. 6.)

One can see that this intuition that error mitigation does not increase the distinguishability is indeed right by looking at the whole error-mitigation process as a quantum channel. Then, the data-processing inequality implies that the distinguishability between any two states should not be increased by the application of quantum channels. This motivates us to rather use this observation as a basis to put a lower bound for the necessary overhead.

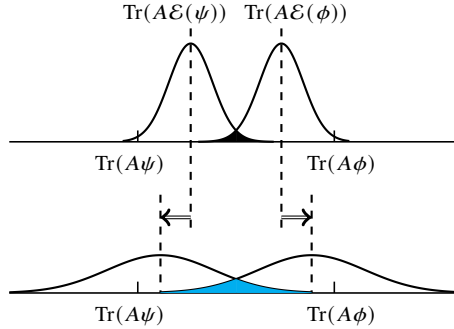


FIG. 6. The top schematic illustrates the probability distribution of an observable A for two noisy states $\mathcal{E}(\psi)$ and $\mathcal{E}(\phi)$. The expectation values are shifted from the true values due to the noise effects. As in the bottom schematic, error mitigation converts them to other distributions whose expectation values are closer to the true values than the initial noisy distributions are. However, the converted distributions get broader, and the overlap between two distributions increases in general.

Appendix B: Proof of Theorem 1

Proof. To show our result, it is useful to formalize the mitigation process as a quantum operation. Since POVM measurements in different experiments are independent of each other, the whole measurement process can be represented as a tensor product of each POVM. Then, the classical post-processing following the measurement is a classical-classical channel such that the expected value of the output will serve as an estimate of the desired expectation value. We can then formalize an error-mitigation process as a concatenation of these two maps.

Definition 4 ((Q, K) -error mitigation). For an arbitrary observable A satisfying $-\mathbb{I}/2 \leq A \leq \mathbb{I}/2$, a (Q, K) -mitigation protocol — involving Q inputs and K experiments — is a concatenation of quantum-classical channel Λ_A and classical-classical channel $\hat{\epsilon}_A$ as $\hat{\epsilon}_A \circ \Lambda_A$. Here, Λ_A has a form

$$\Lambda_A(\cdot) = \sum_{i^{(1)} \dots i^{(K)}} \text{Tr}(\cdot M_{i^{(1)}}^{(1)} \otimes \dots \otimes M_{i^{(K)}}^{(K)}) |i^{(1)} \dots i^{(K)}\rangle\langle i^{(1)} \dots i^{(K)}| \quad (\text{B1})$$

where $\{M_{i^{(k)}}^{(k)}\}$ is the POVM for the k^{th} experiment acting on Q copies of N -qubit noisy states, while $\hat{\epsilon}_A$

implements a K -input classical function e_A such that

$$\sum_{i^{(1)} \dots i^{(K)}} p_{i^{(1)} \dots i^{(K)}} e_A(i^{(1)}, \dots, i^{(K)}) = \text{Tr}(A\psi) + b_A(\psi), \quad (\text{B2})$$

where

$$p_{i^{(1)} \dots i^{(K)}} := \prod_{k=1}^K \text{Tr}[\mathcal{E}_1^{(k)}(\psi) \otimes \dots \otimes \mathcal{E}_Q^{(k)}(\psi) M_{i^{(k)}}^{(k)}] \quad (\text{B3})$$

is the probability of getting outcome $i^{(1)} \dots i^{(K)}$ for the input noisy states $\{\mathcal{E}_q^{(k)}(\psi)\}_{q=1, k=1}^{Q, K}$ and $b_A(\psi)$ is the bias.

We also summarize the general error-mitigation procedure as an algorithm in Table I.

Algorithm (Q, K) -error mitigation	
Input:	Distorted states $\{\mathcal{E}_q^{(k)}(\psi)\}_{q=1, k=1}^{Q, K}$
Output:	Estimate of $\text{Tr}(A\psi)$
1: for $m = 1$ to M do	
2: for $k = 1$ to K do	
3: Input $\mathcal{E}_1^{(k)}(\psi), \dots, \mathcal{E}_Q^{(k)}(\psi)$ into a quantum circuit for error mitigation.	
4: Perform a POVM measurement $\{M_{i^{(k)}}^{(k)}\}$ for the output state and get an outcome $i^{(k)}$.	
5: end for	
6: Using the series of outputs $i^{(1)}, \dots, i^{(K)}$ as an input, apply a classical post-processing to obtain an estimate $e_{A,m} := e_A(i^{(1)}, \dots, i^{(K)})$.	
7: end for	
8: return $\frac{1}{M} \sum_{m=1}^M e_{A,m}$.	

TABLE I. General procedure of (Q, K) -error mitigation.

Let us now recall that the trace distance admits the following form

$$\begin{aligned} D_{\text{tr}}(\rho, \sigma) &= \frac{1}{2} \|\rho - \sigma\|_1 \\ &= \max_{0 \leq M \leq \mathbb{I}} \text{Tr}[M(\rho - \sigma)], \end{aligned} \quad (\text{B4})$$

and similarly the local distinguishability measure can be written as [38]

$$\begin{aligned} D_{\text{LM}}(\rho, \sigma) &= \max_{\{M_i\} \in \text{LM}} \frac{1}{2} \|\mathcal{M}(\rho) - \mathcal{M}(\sigma)\|_1 \\ &= \max_{\{M, \mathbb{I} - M\} \in \text{LM}_2} \text{Tr}[M(\rho - \sigma)] \end{aligned} \quad (\text{B5})$$

where LM is the set of POVMs that take the form $M_{i^{(1)}}^{(1)} \otimes \dots \otimes M_{i^{(K)}}^{(K)}$, where $M_{i^{(k)}}^{(k)}$ represents some POVM local to system S_k , and LM_2 is the set of two-outcome measurements realized by local measurements together with classical post-processing. The second forms for the above measures particularly tell that they quantify how well two states can be distinguished by accessible quantum measurements. By definition, it is clear that

$$D_{\text{tr}}(\rho, \sigma) \geq D_{\text{LM}}(\rho, \sigma) \quad (\text{B6})$$

for all state ρ and σ , and the inequality often becomes strict [60, 61].

The local distinguishability measure satisfies the data-processing inequality under all local measurement channels. Namely, for all states ρ and σ defined on a composite system $\otimes_{k=1}^K S_k$, and for an arbitrary

quantum-classical channel $\Lambda(\cdot) = \sum_i \text{Tr} \left(\cdot M_{i^{(1)}}^{(1)} \otimes \cdots \otimes M_{i^{(K)}}^{(K)} \right) |i^{(1)} \dots i^{(K)}\rangle \langle i^{(1)} \dots i^{(K)}|$,

$$\begin{aligned} D_{\text{LM}}(\Lambda(\rho), \Lambda(\sigma)) &= \max_{\mathcal{M} \in \text{LM}} \frac{1}{2} \|\mathcal{M} \circ \Lambda(\rho) - \mathcal{M} \circ \Lambda(\sigma)\|_1 \\ &\leq \max_{\mathcal{M} \in \text{LM}} \frac{1}{2} \|\mathcal{M}(\rho) - \mathcal{M}(\sigma)\|_1 \\ &= D_{\text{LM}}(\rho, \sigma) \end{aligned} \quad (\text{B7})$$

where in the inequality we used that the set of local measurement channels is closed under concatenation.

Since the channel Λ_A in Definition 4 is a local measurement channel, we employ (B7) to get

$$\begin{aligned} D_{\text{LM}} \left(\otimes_{k=1}^K \otimes_{q=1}^Q \mathcal{E}_q^{(k)}(\psi), \otimes_{k=1}^K \otimes_{q=1}^Q \mathcal{E}_q^{(k)}(\phi) \right) &\geq D_{\text{LM}} \left(\Lambda_A \circ \otimes_{k=1}^K \otimes_{q=1}^Q \mathcal{E}_q^{(k)}(\psi), \Lambda_A \circ \otimes_{k=1}^K \otimes_{q=1}^Q \mathcal{E}_q^{(k)}(\phi) \right) \\ &= D_{\text{LM}}(\hat{p}, \hat{q}) \end{aligned} \quad (\text{B8})$$

where

$$\begin{aligned} \hat{p} &= \sum_{i^{(1)} \dots i^{(K)}} p_{i^{(1)} \dots i^{(K)}} |i^{(1)} \dots i^{(K)}\rangle \langle i^{(1)} \dots i^{(K)}| \\ \hat{q} &= \sum_{i^{(1)} \dots i^{(K)}} q_{i^{(1)} \dots i^{(K)}} |i^{(1)} \dots i^{(K)}\rangle \langle i^{(1)} \dots i^{(K)}| \end{aligned} \quad (\text{B9})$$

and $p_{i^{(1)} \dots i^{(K)}}$ and $q_{i^{(1)} \dots i^{(K)}}$ are classical distributions defined in (B3) for ψ and ϕ respectively, which satisfy

$$\begin{aligned} \sum_{i^{(1)} \dots i^{(K)}} p_{i^{(1)} \dots i^{(K)}} e_A(i^{(1)}, \dots, i^{(K)}) &= \text{Tr}(A\psi) + b_A(\psi), \\ \sum_{i^{(1)} \dots i^{(K)}} q_{i^{(1)} \dots i^{(K)}} e_A(i^{(1)}, \dots, i^{(K)}) &= \text{Tr}(A\phi) + b_A(\phi). \end{aligned} \quad (\text{B10})$$

When \hat{p} and \hat{q} are tensor products of classical states, i.e., $\hat{p} = \hat{p}^{(1)} \otimes \cdots \otimes \hat{p}^{(K)}$ and $\hat{q} = \hat{q}^{(1)} \otimes \cdots \otimes \hat{q}^{(K)}$, it holds that

$$D_{\text{LM}}(\hat{p}, \hat{q}) = D_{\text{tr}}(\hat{p}, \hat{q}). \quad (\text{B11})$$

This can be seen as follows. Let M^* be the optimal POVM element achieving the trace distance in (B4). Then, we get

$$\begin{aligned} D_{\text{tr}}(\hat{p}, \hat{q}) &= \text{Tr}[M^*(\hat{p} - \hat{q})] \\ &= \text{Tr}[\Delta(M^*)(\hat{p} - \hat{q})] \end{aligned} \quad (\text{B12})$$

where

$$\Delta(\cdot) := \sum_{i^{(1)} \dots i^{(K)}} |i^{(1)} \dots i^{(K)}\rangle \langle i^{(1)} \dots i^{(K)}| \cdot |i^{(1)} \dots i^{(K)}\rangle \langle i^{(1)} \dots i^{(K)}| \quad (\text{B13})$$

is a classical dephasing channel. The effective POVM element $\Delta(M^*)$ has the form

$$\Delta(M^*) = \sum_{i^{(1)} \dots i^{(K)}} \langle i^{(1)} \dots i^{(K)} | M^* | i^{(1)} \dots i^{(K)} \rangle |i^{(1)} \dots i^{(K)}\rangle \langle i^{(1)} \dots i^{(K)}|. \quad (\text{B14})$$

Since each $|i^{(1)} \dots i^{(K)}\rangle \langle i^{(1)} \dots i^{(K)}|$ is a local POVM element and $0 \leq \langle i^{(1)} \dots i^{(K)} | M^* | i^{(1)} \dots i^{(K)} \rangle \leq 1$ because $0 \leq M^* \leq \mathbb{I}$, the two-outcome measurement $\{\Delta(M^*), \mathbb{I} - \Delta(M^*)\}$ can be realized by a local measurement and classical post-processing, and thus belongs to LM_2 . This, together with (B5), implies $D_{\text{tr}}(\hat{p}, \hat{q}) \leq D_{\text{LM}}(\hat{p}, \hat{q})$, and further combining (B6) gives (B11).

Combining (B8) and (B11) gives

$$D_{\text{tr}}(\hat{p}, \hat{q}) \leq D_{\text{LM}} \left(\otimes_{k=1}^K \otimes_{q=1}^Q \mathcal{E}_q^{(k)}(\psi), \otimes_{k=1}^K \otimes_{q=1}^Q \mathcal{E}_q^{(k)}(\phi) \right). \quad (\text{B15})$$

We now connect (B15) to the expression (B10) of the expectation value and bias. Let us first suppose $\text{Tr}(A\psi) + b_A(\psi) \geq \text{Tr}(A\phi) + b_A(\phi)$. Let $\mathcal{I}^* := \left\{ (i^{(1)} \dots i^{(K)}) \mid p_{i^{(1)} \dots i^{(K)}} - q_{i^{(1)} \dots i^{(K)}} \geq 0 \right\}$ and let $\bar{\mathcal{I}}^*$ be the

complement set. Let us also define $A' = A + \mathbb{I}/2$, which satisfies $0 \leq A' \leq \mathbb{I}$ due to $-\mathbb{I}/2 \leq A \leq \mathbb{I}/2$. Then, we get

$$\begin{aligned}
\text{Tr}[A'(\psi - \phi)] + b_A(\psi) - b_A(\phi) &= \text{Tr}[(A + \mathbb{I}/2)(\phi - \psi)] + b_A(\phi) - b_A(\psi) \\
&= \text{Tr}[A(\phi - \psi)] + b_A(\phi) - b_A(\psi) \\
&= \sum_{i^{(1)} \dots i^{(K)}} (p_{i^{(1)} \dots i^{(K)}} - q_{i^{(1)} \dots i^{(K)}}) e_A(i^{(1)}, \dots, i^{(K)}) \\
&\leq \sum_{(i^{(1)} \dots i^{(K)}) \in \mathcal{I}^*} (p_{i^{(1)} \dots i^{(K)}} - q_{i^{(1)} \dots i^{(K)}}) e_{A,\max} \\
&\quad + \sum_{(i^{(1)} \dots i^{(K)}) \in \tilde{\mathcal{I}}^*} (p_{i^{(1)} \dots i^{(K)}} - q_{i^{(1)} \dots i^{(K)}}) e_{A,\min} \\
&= D_{\text{tr}}(\hat{p}, \hat{q})(e_{A,\max} - e_{A,\min})
\end{aligned} \tag{B16}$$

where in the third line we used (B10), in the fourth line we used the maximum and minimum estimator values

$$e_{A,\max} := \max_{i^{(1)} \dots i^{(K)}} e_A(i^{(1)} \dots i^{(K)}), \quad e_{A,\min} := \min_{i^{(1)} \dots i^{(K)}} e_A(i^{(1)} \dots i^{(K)}), \tag{B17}$$

and in the last line we used that

$$\sum_{i^{(1)} \dots i^{(K)} \in \tilde{\mathcal{I}}^*} (p_{i^{(1)} \dots i^{(K)}} - q_{i^{(1)} \dots i^{(K)}}) = - \sum_{i^{(1)} \dots i^{(K)} \in \mathcal{I}^*} (p_{i^{(1)} \dots i^{(K)}} - q_{i^{(1)} \dots i^{(K)}}) \tag{B18}$$

and that the trace distance reduces to the total variation distance

$$D_{\text{tr}}(\hat{p}, \hat{q}) = \sum_{i: p_i - q_i \geq 0} (p_i - q_i) \tag{B19}$$

for all classical states $\hat{p} = \sum_i p_i |i\rangle\langle i|$ and $\hat{q} = \sum_i q_i |i\rangle\langle i|$. Combining (B15) and (B16), we get

$$e_{A,\max} - e_{A,\min} \geq \frac{\text{Tr}[A'(\psi - \phi)] + b_A(\psi) - b_A(\phi)}{D_{\text{LM}}\left(\otimes_{k=1}^K \otimes_{q=1}^Q \mathcal{E}_q^{(k)}(\psi), \otimes_{k=1}^K \otimes_{q=1}^Q \mathcal{E}_q^{(k)}(\phi)\right)}. \tag{B20}$$

On the other hand, if $\text{Tr}(A\psi) + b_A(\psi) \leq \text{Tr}(A\phi) + b_A(\phi)$, we flip the role of ψ and ϕ to get

$$e_{A,\max} - e_{A,\min} \geq - \frac{\text{Tr}[A'(\psi - \phi)] + b_A(\psi) - b_A(\phi)}{D_{\text{LM}}\left(\otimes_{k=1}^K \otimes_{q=1}^Q \mathcal{E}_q^{(k)}(\psi), \otimes_{k=1}^K \otimes_{q=1}^Q \mathcal{E}_q^{(k)}(\phi)\right)}. \tag{B21}$$

These two can be summarized as

$$e_{A,\max} - e_{A,\min} \geq \frac{|\text{Tr}[A'(\psi - \phi)] + b_A(\psi) - b_A(\phi)|}{D_{\text{LM}}\left(\otimes_{k=1}^K \otimes_{q=1}^Q \mathcal{E}_q^{(k)}(\psi), \otimes_{k=1}^K \otimes_{q=1}^Q \mathcal{E}_q^{(k)}(\phi)\right)}. \tag{B22}$$

Optimizing over A , ϕ , and ψ on both sides, we reach

$$\begin{aligned}
\Delta e_{\max} &\geq \max_{\psi, \phi \atop -\mathbb{I}/2 \leq A \leq \mathbb{I}/2} \frac{|\text{Tr}[A'(\psi - \phi)] + b_A(\psi) - b_A(\phi)|}{D_{\text{LM}}\left(\otimes_{k=1}^K \otimes_{q=1}^Q \mathcal{E}_q^{(k)}(\psi), \otimes_{k=1}^K \otimes_{q=1}^Q \mathcal{E}_q^{(k)}(\phi)\right)} \\
&= \max_{\psi, \phi \atop -\mathbb{I}/2 \leq A \leq \mathbb{I}/2} \frac{\text{Tr}[A'(\psi - \phi)] + b_A(\psi) - b_A(\phi)}{D_{\text{LM}}\left(\otimes_{k=1}^K \otimes_{q=1}^Q \mathcal{E}_q^{(k)}(\psi), \otimes_{k=1}^K \otimes_{q=1}^Q \mathcal{E}_q^{(k)}(\phi)\right)} \\
&\geq \max_{\psi, \phi} \frac{D_{\text{tr}}(\psi, \phi) + b_{A^*}(\psi) - b_{A^*}(\phi)}{D_{\text{LM}}\left(\otimes_{k=1}^K \otimes_{q=1}^Q \mathcal{E}_q^{(k)}(\psi), \otimes_{k=1}^K \otimes_{q=1}^Q \mathcal{E}_q^{(k)}(\phi)\right)} \\
&\geq \max_{\psi, \phi} \frac{D_{\text{tr}}(\psi, \phi) - 2b_{\max}}{D_{\text{LM}}\left(\otimes_{k=1}^K \otimes_{q=1}^Q \mathcal{E}_q^{(k)}(\psi), \otimes_{k=1}^K \otimes_{q=1}^Q \mathcal{E}_q^{(k)}(\phi)\right)}
\end{aligned} \tag{B23}$$

where in the second line we used that we can always take the numerator positive by appropriately flipping ψ and ϕ , in the third line we fixed $A'^* = A^* + \mathbb{I}/2$ to the one that achieves the trace distance $\text{Tr}[A'^*(\psi - \phi)] = D_{\text{tr}}(\psi, \phi)$ as in (B4), and in the fourth line we used the definition of b_{\max} . \square

Appendix C: Proof of Theorem 3

Proof. For an arbitrary unitary channel \mathcal{V} , Eq. (3) in Theorem 1 can also be written as

$$\begin{aligned}
\Delta e_{\max} &\geq \max_{\psi, \phi} \frac{D_{\text{tr}}(\psi, \phi) - 2b_{\max}}{D_{\text{LM}}\left(\otimes_{k=1}^K \otimes_{q=1}^Q \mathcal{E}_q^{(k)}(\psi), \otimes_{k=1}^K \otimes_{q=1}^Q \mathcal{E}_q^{(k)}(\phi)\right)} \\
&= \max_{\psi, \phi} \frac{D_{\text{tr}}(\mathcal{V}^\dagger(\psi), \mathcal{V}^\dagger(\phi)) - 2b_{\max}}{D_{\text{LM}}\left(\otimes_{k=1}^K \otimes_{q=1}^Q \mathcal{E}_q^{(k)} \circ \mathcal{V}(\mathcal{V}^\dagger(\psi)), \otimes_{k=1}^K \otimes_{q=1}^Q \mathcal{E}_q^{(k)} \circ \mathcal{V}(\mathcal{V}^\dagger(\phi))\right)} \\
&= \max_{\psi_{\text{in}}, \phi_{\text{in}}} \frac{D_{\text{tr}}(\psi_{\text{in}}, \phi_{\text{in}}) - 2b_{\max}}{D_{\text{LM}}\left(\otimes_{k=1}^K \otimes_{q=1}^Q \mathcal{E}_q^{(k)} \circ \mathcal{V}(\psi_{\text{in}}), \otimes_{k=1}^K \otimes_{q=1}^Q \mathcal{E}_q^{(k)} \circ \mathcal{V}(\phi_{\text{in}})\right)},
\end{aligned} \tag{C1}$$

where in the second line we used the unitary invariance of the trace distance, and in the third line we changed the variables as $\mathcal{V}^\dagger(\psi) \rightarrow \psi_{\text{in}}$, $\mathcal{V}^\dagger(\phi) \rightarrow \phi_{\text{in}}$ and used the fact that the application of a fixed unitary does not affect the optimization taken over all states.

The noise model for layered circuits typically assumes the application of a noise channel after each layer. Let $\mathcal{N}_{q,l}^{(k)}$ be a noise channel after the l^{th} layer for the q^{th} input in the k^{th} experiment. Then, a noisy circuit for the q^{th} input in the k^{th} experiment is described by

$$\mathcal{N}_{q,L}^{(k)} \circ \mathcal{U}_L \circ \cdots \circ \mathcal{N}_{q,1}^{(k)} \circ \mathcal{U}_1 \tag{C2}$$

while the ideal output given input state ψ_{in} is $\psi = \mathcal{U}_L \circ \cdots \circ \mathcal{U}_1(\psi_{\text{in}})$. The effective noise channel for the q^{th} input in the k^{th} experiment is then given by

$$\mathcal{E}_q^{(k)} = \mathcal{N}_{q,L}^{(k)} \circ \mathcal{U}_L \circ \cdots \circ \mathcal{N}_{q,1}^{(k)} \circ \mathcal{U}_1 \circ \mathcal{U}_1^\dagger \circ \mathcal{U}_2^\dagger \circ \cdots \circ \mathcal{U}_L^\dagger. \tag{C3}$$

Plugging (C3) into (C1) while taking $\mathcal{V} = \mathcal{U}_L \circ \cdots \circ \mathcal{U}_1$, we get

$$\Delta e_{\max} \geq \max_{\psi_{\text{in}}, \phi_{\text{in}}} \frac{D_{\text{tr}}(\psi_{\text{in}}, \phi_{\text{in}}) - 2b_{\max}}{D_{\text{LM}}\left(\otimes_{k=1}^K \otimes_{q=1}^Q \prod_{l=1}^L [\mathcal{N}_{q,l}^{(k)} \circ \mathcal{U}_l](\psi_{\text{in}}), \otimes_{k=1}^K \otimes_{q=1}^Q \prod_{l=1}^L [\mathcal{N}_{q,l}^{(k)} \circ \mathcal{U}_l](\phi_{\text{in}})\right)}, \tag{C4}$$

where we used the notation

$$\prod_{l=1}^L [\mathcal{N}_{q,l}^{(k)} \circ \mathcal{U}_l] := \mathcal{N}_{q,L}^{(k)} \circ \mathcal{U}_L \circ \cdots \circ \mathcal{N}_{q,1}^{(k)} \circ \mathcal{U}_1 \tag{C5}$$

The denominator of the right-hand side of (C4) can be bounded as

$$\begin{aligned}
&D_{\text{LM}}\left(\otimes_{k=1}^K \otimes_{q=1}^Q \prod_{l=1}^L [\mathcal{N}_{q,l}^{(k)} \circ \mathcal{U}_l](\psi_{\text{in}}), \otimes_{k=1}^K \otimes_{q=1}^Q \prod_{l=1}^L [\mathcal{N}_{q,l}^{(k)} \circ \mathcal{U}_l](\phi_{\text{in}})\right) \\
&\leq D_{\text{tr}}\left(\otimes_{k=1}^K \otimes_{q=1}^Q \prod_{l=1}^L [\mathcal{N}_{q,l}^{(k)} \circ \mathcal{U}_l](\psi_{\text{in}}), \otimes_{k=1}^K \otimes_{q=1}^Q \prod_{l=1}^L [\mathcal{N}_{q,l}^{(k)} \circ \mathcal{U}_l](\phi_{\text{in}})\right) \\
&\leq D_{\text{tr}}\left(\otimes_{k=1}^K \otimes_{q=1}^Q \prod_{l=1}^L [\mathcal{N}_{q,l}^{(k)} \circ \mathcal{U}_l](\psi_{\text{in}}), \frac{\mathbb{I}}{2^{KQN}}\right) + D_{\text{tr}}\left(\otimes_{k=1}^K \otimes_{q=1}^Q \prod_{l=1}^L [\mathcal{N}_{q,l}^{(k)} \circ \mathcal{U}_l](\phi_{\text{in}}), \frac{\mathbb{I}}{2^{KQN}}\right) \\
&\leq \sum_{k=1}^K \left[D_{\text{tr}}\left(\otimes_{q=1}^Q \prod_{l=1}^L [\mathcal{N}_{q,l}^{(k)} \circ \mathcal{U}_l](\psi_{\text{in}}), \frac{\mathbb{I}}{2^{QN}}\right) + D_{\text{tr}}\left(\otimes_{q=1}^Q \prod_{l=1}^L [\mathcal{N}_{q,l}^{(k)} \circ \mathcal{U}_l](\phi_{\text{in}}), \frac{\mathbb{I}}{2^{QN}}\right) \right]
\end{aligned} \tag{C6}$$

where the first inequality is due to (B6), the second inequality is due to the triangle inequality, and in the last line

we bounded each term by sequentially applying the triangle inequality as

$$\begin{aligned}
& D_{\text{tr}} \left(\otimes_{k=1}^K \otimes_{q=1}^Q \prod_{l=1}^L \left[\mathcal{N}_{q,l}^{(k)} \circ \mathcal{U}_l \right] (\psi_{\text{in}}), \frac{\mathbb{I}}{2^{KQN}} \right) \\
& \leq D_{\text{tr}} \left(\otimes_{k=1}^K \otimes_{q=1}^Q \prod_{l=1}^L \left[\mathcal{N}_{q,l}^{(k)} \circ \mathcal{U}_l \right] (\psi_{\text{in}}), \frac{\mathbb{I}}{2^{QN}} \otimes_{k=2}^K \otimes_{q=1}^Q \prod_{l=1}^L \left[\mathcal{N}_{q,l}^{(k)} \circ \mathcal{U}_l \right] (\psi_{\text{in}}) \right) \\
& \quad + D_{\text{tr}} \left(\frac{\mathbb{I}}{2^{QN}} \otimes_{k=2}^K \otimes_{q=1}^Q \prod_{l=1}^L \left[\mathcal{N}_{q,l}^{(k)} \circ \mathcal{U}_l \right] (\psi_{\text{in}}), \frac{\mathbb{I}}{2^{QN}} \otimes \frac{\mathbb{I}}{2^{QN(K-1)}} \right) \\
& = D_{\text{tr}} \left(\otimes_{q=1}^Q \prod_{l=1}^L \left[\mathcal{N}_{q,l}^{(1)} \circ \mathcal{U}_l \right] (\psi_{\text{in}}), \frac{\mathbb{I}}{2^{QN}} \right) + D_{\text{tr}} \left(\otimes_{k=2}^K \otimes_{q=1}^Q \prod_{l=1}^L \left[\mathcal{N}_{q,l}^{(k)} \circ \mathcal{U}_l \right] (\psi_{\text{in}}), \frac{\mathbb{I}}{2^{QN(K-1)}} \right) \\
& \leq \dots \\
& \leq \sum_{k=1}^K D_{\text{tr}} \left(\otimes_{q=1}^Q \prod_{l=1}^L \left[\mathcal{N}_{q,l}^{(k)} \circ \mathcal{U}_l \right] (\psi_{\text{in}}), \frac{\mathbb{I}}{2^{QN}} \right),
\end{aligned} \tag{C7}$$

and similarly for the second term. The last expression in (C6) can be further upper bounded as

$$\leq \sqrt{\frac{\ln 2}{2}} \sum_{k=1}^K \left(\sqrt{S \left(\otimes_{q=1}^Q \prod_{l=1}^L \left[\mathcal{N}_{q,l}^{(k)} \circ \mathcal{U}_l \right] (\psi_{\text{in}}) \middle\| \frac{\mathbb{I}}{2^{QN}} \right)} + \sqrt{S \left(\otimes_{q=1}^Q \prod_{l=1}^L \left[\mathcal{N}_{q,l}^{(k)} \circ \mathcal{U}_l \right] (\phi_{\text{in}}) \middle\| \frac{\mathbb{I}}{2^{QN}} \right)} \right), \tag{C8}$$

where we used the quantum Pinsker's inequality [62]

$$D_{\text{tr}}(\rho, \sigma) \leq \sqrt{\frac{\ln 2}{2}} \sqrt{S(\rho \parallel \sigma)} \tag{C9}$$

for all states ρ, σ , where $S(\rho \parallel \sigma) := \text{Tr}(\rho \log \rho) - \text{Tr}(\rho \log \sigma)$ is the relative entropy.

We now recall Theorem 6.1 of Ref. [42] (see also Supplementary Lemma 5 of Ref. [27]), which evaluates the entropy increase due to the local depolarizing noise.

Lemma 5 ([42]). *Let $\mathcal{D}_\epsilon^d(\rho) = (1 - \epsilon)\rho + \epsilon\mathbb{I}/d$ be a d -dimensional depolarizing channel. Then, for an arbitrary n -qudit state ρ_n , it holds that*

$$S \left(\left(\mathcal{D}_\epsilon^d \right)^{\otimes n} (\rho_n) \middle\| \mathbb{I}/d^n \right) \leq (1 - \epsilon)S(\rho_n \parallel \mathbb{I}/d^n). \tag{C10}$$

Then, for $\mathcal{N}_{q,l}^{(k)} = \mathcal{D}_{\epsilon_k}^{\otimes N}$ where \mathcal{D}_{ϵ_k} is a qubit depolarizing channel (see also Fig. 7), we get

$$\begin{aligned}
S \left(\otimes_{q=1}^Q \prod_{l=1}^L \left[\mathcal{N}_{q,l}^{(k)} \circ \mathcal{U}_l \right] (\psi_{\text{in}}) \middle\| \frac{\mathbb{I}}{2^{QN}} \right) &= S \left(\prod_{l=1}^L \left[\mathcal{D}_{\epsilon_k}^{\otimes QN} \circ \mathcal{U}_l^{\otimes Q} \right] (\psi_{\text{in}}^{\otimes Q}) \middle\| \frac{\mathbb{I}}{2^{QN}} \right) \\
&\leq (1 - \epsilon_k) S \left(\mathcal{U}_L^{\otimes Q} \prod_{l=2}^L \left[\mathcal{D}_{\epsilon_k}^{\otimes QN} \circ \mathcal{U}_l^{\otimes Q} \right] (\psi_{\text{in}}^{\otimes Q}) \middle\| \frac{\mathbb{I}}{2^{QN}} \right) \\
&= (1 - \epsilon_k) S \left(\prod_{l=2}^L \left[\mathcal{D}_{\epsilon_k}^{\otimes QN} \circ \mathcal{U}_l^{\otimes Q} \right] (\psi_{\text{in}}^{\otimes Q}) \middle\| \frac{\mathbb{I}}{2^{QN}} \right) \\
&\leq (1 - \epsilon_k)^L S \left(\psi_{\text{in}}^{\otimes Q} \middle\| \frac{\mathbb{I}}{2^{QN}} \right) \\
&\leq (1 - \epsilon_k)^L QN,
\end{aligned} \tag{C11}$$

where the second line follows from Lemma 5, the third line is due to the unitary invariance of the relative entropy, in the fourth line we sequentially applied the same argument for L times, and the fifth line is from the upper bound of the relative entropy, which is saturated by pure state ψ_{in} .

Using (C11), we can put a further bound on (C8) as

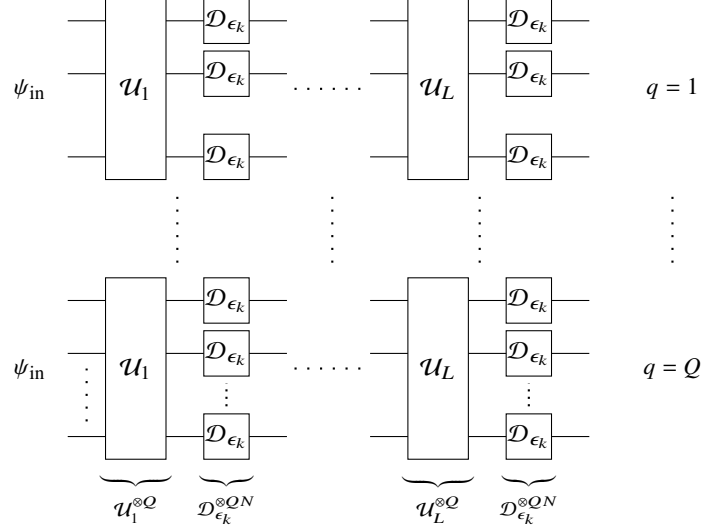


FIG. 7. Noisy layered circuit for the k^{th} experiment under local depolarizing noise \mathcal{D}_{ϵ_k} . Each experiment contains Q copies of the noisy circuit.

$$\begin{aligned} &\leq \sqrt{2 \ln 2} \sqrt{QN} \sum_{k=1}^K (1 - \epsilon_k)^{L/2} \\ &\leq \sqrt{2 \ln 2} \sqrt{QN} K (1 - \epsilon_{\min})^{L/2}, \end{aligned} \quad (\text{C12})$$

where $\epsilon_{\min} := \min_k \epsilon_k$. This evaluates the lower bound of (C4) as

$$\Delta e_{\max} \geq \max_{\psi_{\text{in}}, \phi_{\text{in}}} \frac{D_{\text{tr}}(\psi_{\text{in}}, \phi_{\text{in}}) - 2b_{\max}}{\sqrt{2 \ln 2} \sqrt{QN} K} \left(\frac{1}{1 - \epsilon_{\min}} \right)^{L/2}. \quad (\text{C13})$$

Noting $\max_{\psi_{\text{in}}, \phi_{\text{in}}} D_{\text{tr}}(\psi_{\text{in}}, \phi_{\text{in}}) = 1$ concludes the proof. \square

Appendix D: Details on specific error-mitigation protocols

1. Richardson extrapolation

Extrapolation methods [12, 13] are used in scenarios where there is no clear analytical noise model. These strategies consider a family of noise channels $\{\mathcal{N}_{\xi}\}_{\xi}$, where ξ corresponds to the noise strength. The assumption here is that the description of \mathcal{N}_{ξ} is unknown, but we have the ability to “boost” ξ such that $\xi \geq \tilde{\xi}$ where $\tilde{\xi}$ is the noise strength present in some given noisy circuit. The idea is that by studying how the expectation value of an observable depends on ξ , we can extrapolate what its value would be if $\xi = 0$. In particular, the R^{th} order Richardson extrapolation method work as follows. Let us take constants $\{\gamma_r\}_{r=0}^R$ and $\{c_r\}_{r=0}^R$ such that

$$\sum_{r=0}^R \gamma_r = 1, \quad \sum_{r=0}^R \gamma_r c_r^t = 0 \quad t = 1, \dots, R. \quad (\text{D1})$$

Using these constants, one can show that

$$\sum_{r=0}^R \gamma_r \text{Tr}[A \mathcal{N}_{c_r \tilde{\xi}}(\psi)] = \text{Tr}(A\psi) + b_A(\psi) \quad (\text{D2})$$

where $b_A(\psi) = O(\tilde{\xi}^{R+1})$. This allows us to estimate the true expectation value using noisy states under multiple noise levels, as long as $\tilde{\xi}$ is sufficiently small.

Richardson extrapolation is an instance of $(1, R+1)$ -error mitigation. In particular, we have

$$\mathcal{E}^{(k)} = \mathcal{N}_{c_{k-1} \tilde{\xi}} \quad k = 1, \dots, R+1 \quad (\text{D3})$$

in Definition 4. For an observable $A = \sum_a a \Pi_a$ where Π_a is the projector corresponding to measuring outcome a , the POVMs $\{M_{a^{(k)}}^{(k)}\}_{k=1}^{R+1}$ and classical estimator function e_A take the forms

$$M_{a^{(k)}}^{(k)} = \Pi_{a^{(k)}} \quad k = 1, \dots, R+1, \quad (\text{D4})$$

$$e_A(a^{(1)}, \dots, a^{(R+1)}) = \sum_{k=1}^{R+1} \gamma_{k-1} a^{(k)}, \quad (\text{D5})$$

where $\{\gamma_k\}_{k=0}^R$ are the constants determined by (D1). One can easily check that plugging the above expressions in the form of Definition 4 leads to (D2).

Because of the constraint $-\mathbb{I}/2 \leq A \leq \mathbb{I}/2$, every eigenvalue a satisfies $-1/2 \leq a \leq 1/2$. This implies that

$$\begin{aligned} e_{A,\max} &\leq \frac{1}{2} \sum_{r: \gamma_r \geq 0} \gamma_r - \frac{1}{2} \sum_{r: \gamma_r < 0} \gamma_r \\ &= \frac{1}{2} \sum_{r=0}^R |\gamma_r| \end{aligned} \quad (\text{D6})$$

and

$$\begin{aligned} e_{A,\min} &\geq -\frac{1}{2} \sum_{r: \gamma_r \geq 0} \gamma_r + \frac{1}{2} \sum_{r: \gamma_r < 0} \gamma_r \\ &= -\frac{1}{2} \sum_{r=0}^R |\gamma_r|, \end{aligned} \quad (\text{D7})$$

leading to $\Delta e_{\max} \leq \sum_{r=0}^R |\gamma_r|$. On the other hand, any observable A having $\pm 1/2$ eigenvalues saturates this inequality. Therefore, we get the exact expression of the maximum spread for the extrapolation method as

$$\Delta e_{\max}^{\text{EX}} = \sum_{r=0}^R |\gamma_r|. \quad (\text{D8})$$

Similarly to probabilistic error cancellation, we also compare the actual spread and the lower bound from Theorem 1 for the 3-qubit hardware-efficient ansatz circuits (Fig. 8). Here, we consider the second order Richardson extrapolation, i.e., $R = 2$ and $K = 3$, where we set $c_r = 2^r$. Since the strategy only depends on $\{\gamma_r\}$ and the observable A , the spread is completely determined once R and $\{c_r\}$ are fixed. An important difference from probabilistic error cancellation is that the estimation given by Richardson extrapolation is not unbiased, i.e., $b_{\max} \neq 0$. To make a fair comparison between the actual spread for noise extrapolation and our lower bound, we plot the lower bound using the bias that comes with Richardson extrapolation for each number of layers; see Appendix E for details. In addition, since the ultimate goal of error mitigation is to realize $b_{\max} = 0$, we also plot the lower bound corresponding to $b_{\max} = 0$ to provide an ultimate bound that the spread would need to satisfy if the mitigation protocol achieved unbiased estimation.

We can see that the unbiased lower bound particularly shows an exponential growth with the circuit depth, quickly approaching the actual spread and even surpassing the actual spread in the large depth regime. This indicates a severe restriction incurred on all unbiased estimators, which noise extrapolation fails to satisfy. On the other hand, the biased lower bound shows a saturating trend with the number of layers. This is because extrapolation suffers from a greater bias with a larger accumulated noise [63], and correspondingly the lower bound with respect to the same bias function is pushed down as the circuit depth increases. We can also observe that the peculiar behavior of the actual spread — being constant regardless of the circuit depth — causes the massive inefficiency in the small-depth regime. This is due to the specific property of extrapolation that it does not utilize the knowledge of effective noise channels. These observations suggest that extrapolation can have much room for improvement in the extensive range of accumulated noise strength.

2. Virtual distillation

Virtual distillation [21, 22] is an example of $(Q, 1)$ -error mitigation. Let ψ be an ideal pure output state from a quantum circuit. We consider a scenario where the noise in the circuit acts as an effective noise channel \mathcal{E} that

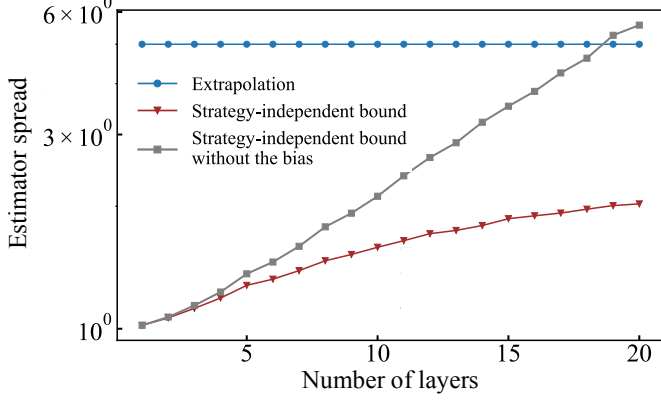


FIG. 8. **Performance of Richardson extrapolation for a layered circuit.** The strategy-independent lower bound with/without bias for $Q = 1$, $K = 3$ (brown triangles/gray squares) and the spread for the second-order Richardson extrapolation (blue dots). Each data point of the strategy-independent bound was obtained by evaluating 10^2 pairs of output states from a noisy hardware-efficient ansatz circuit and taking the maximum value that gives the tightest bounds. We see that the allowance of bias significantly affects the optimal lower bound.

brings the ideal state to a noisy state of the form

$$\mathcal{E}(\psi) = \lambda\psi + \sum_{k=2}^d \lambda_k \psi_k \quad (D9)$$

for a certain $\{\lambda_k\}_{k=1}^d$ with $\lambda_1 := \lambda > 1/2$, where d is the dimension of the system and $\{\psi_k\}_{k=1}^d$ constructs an orthonormal basis with $\psi_1 := \psi$. This form reflects the intuition that, as long as the noise is sufficiently small, the dominant eigenvector should be close to the ideal state ψ . For a more detailed analysis of the form of this spectrum, we refer readers to Ref. [64].

The Q -copy virtual distillation algorithm aims to estimate $\text{Tr}(W\psi)$ for a unitary observable W satisfying $W^2 = \mathbb{I}$ (e.g., Pauli operators) by using Q copies of $\mathcal{E}(\psi)$. The mitigation circuit consists of a controlled permutation and unitary W , followed by a measurement on the control qubit with the Hadamard basis. The probability of getting outcome 0 (projecting onto $|+\rangle\langle+|$) is

$$\begin{aligned} p_0 &= \frac{1}{2} \left(1 + \text{Tr} [W\mathcal{E}(\psi)^Q] \right) \\ &= \frac{1}{2} \left[1 + \lambda^Q \text{Tr}(W\psi) + \sum_{k=2}^d \lambda_k^Q \text{Tr}(W\psi_k) \right]. \end{aligned} \quad (D10)$$

This implies that

$$(2p_0 - 1)\lambda^{-Q} = \text{Tr}(W\psi) + \sum_{k=2}^d \left(\frac{\lambda_k}{\lambda} \right)^Q \text{Tr}(W\psi_k), \quad (D11)$$

providing a way of estimating $\text{Tr}(W\psi)$ with the bias $|\sum_{k=2}^d (\lambda_k/\lambda)^Q \text{Tr}(W\psi_k)| \leq \sum_{k=2}^d (\lambda_k/\lambda)^Q$.

We can see that this protocol fits into our framework with $K = 1$ and $\mathcal{E}_q = \mathcal{E}$ for $q = 1, \dots, Q$ as follows. For an arbitrary observable A with $-\mathbb{I}/2 \leq A \leq \mathbb{I}/2$, we can always find a decomposition with respect to the Pauli operators $\{P_i\}$ as

$$A = \sum_i c_i P_i \quad (D12)$$

for some set of real numbers $\{c_i\}$. We now apply the virtual distillation circuit for P_i at probability $|c_i|/\sum_j |c_j|$ and — similarly to the case of probabilistic error cancellation — employ an estimator function defined as

$$\begin{aligned} e_A(i0) &:= \gamma \text{sgn}(c_i) \lambda^{-Q} \\ e_A(i1) &:= -\gamma \text{sgn}(c_i) \lambda^{-Q} \end{aligned} \quad (D13)$$

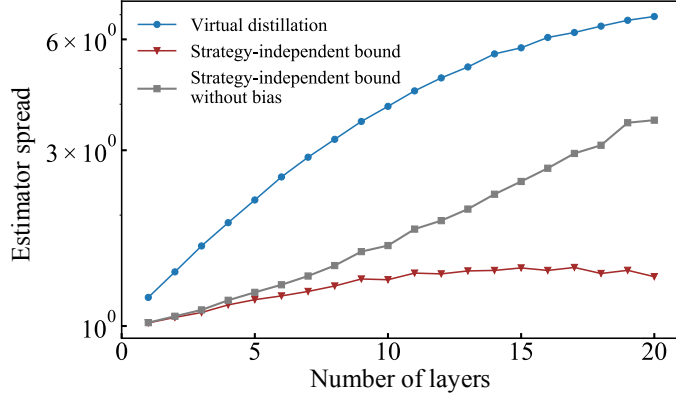


FIG. 9. **Performance of virtual distillation for a layered circuit.** The strategy-independent lower bound with / without bias for $Q = 2$, $K = 1$ (brown triangles / gray squares) and the lower bound $\Delta \tilde{e}_{\max}^{\text{VD}}$ of the spread in (D17) for 2-copy virtual distillation (blue dots). For each layer, we sampled 10^2 pairs of output states from a noisy hardware-efficient ansatz circuit and evaluated the pair that gives the maximum $\Delta \tilde{e}_{\max}^{\text{VD}}$. To compute $\Delta \tilde{e}_{\max}^{\text{VD}}$, we used $\text{Tr} [\mathcal{E}(\psi)^Q]^{-1}$ instead of λ^{-Q} as suggested in Ref. [21].

with $\gamma := \sum_i |c_i|$, where we treat i as a part of the measurement outcome. Then, we get

$$\sum_i [p_{i0} e_A(i0) + p_{i1} e_A(i1)] = \text{Tr}(A\psi) + b_A(\psi) \quad (\text{D14})$$

where p_{i0} is the probability (D10) with $W = P_i$, $p_{i1} = 1 - p_{i0}$, and $b_A(\psi) := \sum_{k=2}^d (\lambda_k / \lambda)^Q \text{Tr}(A\psi_k)$. Optimizing over observables $-\mathbb{I}/2 \leq A \leq \mathbb{I}/2$, we have

$$\Delta e_{\max}^{\text{VD}} = \max \left\{ 2\lambda^{-Q} \sum_i |c_i| \mid -\mathbb{I}/2 \leq \sum_i c_i P_i \leq \mathbb{I}/2 \right\} \quad (\text{D15})$$

and

$$b_{\max}^{\text{VD}} = \sum_{k=2}^d \frac{1}{2} \left(\frac{\lambda_k}{\lambda} \right)^Q. \quad (\text{D16})$$

It is convenient to lower bound the maximum bias (D15) using a simple form as

$$\Delta e_{\max}^{\text{VD}} \geq \Delta \tilde{e}_{\max}^{\text{VD}} := \lambda^{-Q}, \quad (\text{D17})$$

where $\Delta \tilde{e}_{\max}^{\text{VD}}$ is obtained by specifically choosing $c_0 = 1/2$ (with $P_0 := \mathbb{I}$) and $c_i = 0$, $\forall i \neq 0$ in (D15).

Fig. 9 shows the numerical simulation for the 3-qubit hardware-efficient ansatz, comparing the lower bound $\Delta \tilde{e}_{\max}^{\text{VD}}$ of the actual spread and the strategy-independent lower bounds from Theorem 1 with and without bias. Analogously to the case of noise extrapolation, we compute the biased lower bound using the bias that comes with the virtual distillation for each number of layers. As expected, we observe that the actual spread grows with the circuit depth because of the increase in the effective noise strength. The lower bounds show similar behavior to what we observed in Fig. 8; the lower bound without bias shows an exponential growth with the circuit depth, while that with bias saturates in the high noise regime. This is due to a similar mechanism to the case of noise extrapolation, in which the bias gets worse as noise increases.

3. Measuring optimality and future directions

Let us briefly discuss how our bounds could be deployed to benchmark and compare various error mitigation methods. First, observe that probabilistic error cancellation was shown to achieve ultimate performance limits for a certain class of noise. In these situations, it stands optimal among all the error-mitigation strategies —

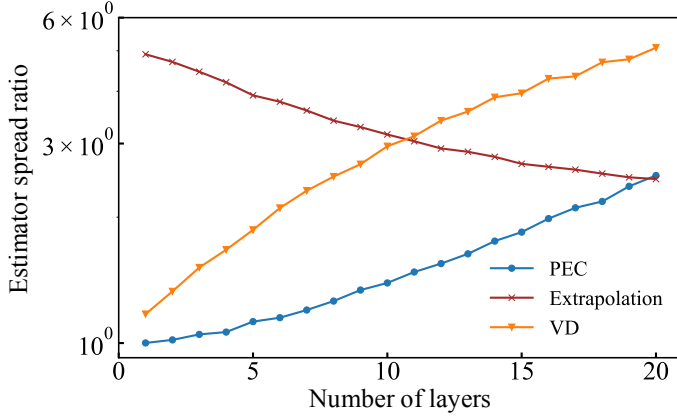


FIG. 10. **Comparison of optimality.** The spread ratio compares the maximum spread for a (Q, K) -mitigation protocol P and the strategy-independent bound for (Q, K) -protocols with the same bias function. We numerically estimate the spread ratio for probabilistic error cancellation with a global operation (PEC), Richardson extrapolation (Extrapolation), and virtual distillation (VD) on a 3-qubit layered circuit with the hardware-efficient ansatz.

including those yet undiscovered. Any protocol that results in a smaller estimator spread without inducing extra bias would necessarily violate the data processing inequality. In more general settings (such as layered circuits) there was always a noticeable difference between the estimator gaps that known error mitigation methods can achieve and our strategy-independent bound, indicating that there may be significant room for improvement.

It is then natural to identify an indicator of this unrealized potential. Consider a particular error-mitigation procedure P with estimator spread Δe_{\max}^P . We can then introduce the spread ratio $r := \Delta e_{\max}^P / \Delta e_{\max}^{\text{all}}$, where $\Delta e_{\max}^{\text{all}}$ is our strategy-independent bound. Thus, $r = 1$ corresponds to an error-mitigation process that is provably optimal, and any $r > 1$ suggests potential room for improvement. In Fig. 10, we numerically estimate the spread ratio for probabilistic error cancellation (blue line), error extrapolation (brown line) and virtual distillation (yellow line) for the 3-qubit layered circuit at various numbers of layers. For a modest number of layers, we see that probabilistic error cancellation appears to be significantly closer to optimal than the other methods. Meanwhile, noise extrapolation appears to better approach optimal limits when the number of layers is large.

We remark, though, that how close an error-mitigation protocol approaches optimal limits is only one measure of its usefulness. Besides the sampling overhead, bias is equally important; an error-mitigation protocol that is perfectly optimal in guessing 0 for any $\text{Tr}(A\psi)$, for example, is not useful at all. Here, probabilistic error cancellation has a significant advantage, as its estimates always have no bias. In comparison, noise extrapolation features bias that tends to grow with the number of layers, which may void the usefulness of its optimality advantage.

On the other hand, a more subtle criterion is the necessity for pre-knowledge. For example, probabilistic error cancellation involves simulation of the inverse noise channel \mathcal{E}^{-1} — which requires complete knowledge of what errors affect our NISQ device. By incorporating this pre-knowledge into the error-mitigation process, it can achieve zero bias. In contrast, noise extrapolation and virtual distillation are designed to be noise-model agnostic. Thus, their increased bias comes with the benefit of additional versatility (e.g., no gate-set tomography required).

These observations suggest that an exciting future direction is to find methods of quantifying such trade-offs. Doing so could point at ways to enhance noise extrapolation or virtual distillation by finding means of partially integrating pre-knowledge. Indeed, recent hybrid approaches [34, 65–67] are equipped with such properties and thus can be good candidates for the optimal strategies. We leave a thorough analysis of these protocols using our framework as potential future work.

Appendix E: Details of numerical simulation

We numerically compare the strategy-independent lower bound derived in this work to the actual spread of prominent mitigation methods, i.e., probabilistic error cancellation, extrapolation, and virtual distillation. We simulate the 3-qubit hardware-efficient ansatz [9] shown in Fig. 11 with various L . Each layer of the ansatz consists of $Y-$, $Z-$ rotation gates, followed by the controlled Z gates; in the numerical simulation, we randomly

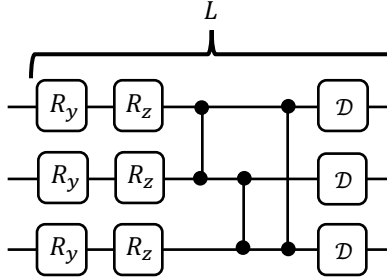


FIG. 11. The hardware-efficient circuit used in the numerical simulation. We fixed $\epsilon = 0.04$ throughout the numerics.

generate the rotation angles $\theta \in [0, 2\pi)$ to prepare the ansatz circuit. We consider the local depolarizing noise model, in which the qubit depolarizing noise

$$\begin{aligned} \mathcal{D}_\epsilon(\rho) &:= (1 - \epsilon)\rho + \epsilon\mathbb{I}/2 \\ &= \left(1 - \frac{3\epsilon}{4}\right)\rho + \frac{\epsilon}{4}(X\rho X + Y\rho Y + Z\rho Z) \end{aligned} \quad (\text{E1})$$

applies to each qubit.

We now explain the lower bounds evaluated in the simulation: the lower bounds with and without bias. The maximum spread is lower bounded as in (B23), but the exact evaluation of the lower bounds is in general intractable. The first problem is that evaluating D_{LM} is computationally demanding in many cases. To circumvent this, we use D_{tr} in place of D_{LM} , which still gives a valid lower bound because the trace distance upper bounds the local distinguishability measure as in (B6). The second problem is that the full optimization over all states ψ and ϕ tends to be prohibitively costly. However, every pair of states ψ and ϕ gives a valid lower bound, so we restrict our attention to intuitive choices, that is, pairs of pure orthogonal states. In particular, we consider orthogonal GHZ states $|\psi_{\text{GHZ}_+}\rangle := \frac{1}{\sqrt{2}}(|0\rangle^{\otimes N} \pm |1\rangle^{\otimes N})$ and generate random input states $\psi_{\text{in}} := \mathcal{U}_{\text{Haar}}(\psi_{\text{GHZ}_+})$ and $\phi_{\text{in}} := \mathcal{U}_{\text{Haar}}(\psi_{\text{GHZ}_-})$, where $\mathcal{U}_{\text{Haar}}$ is an n -qubit Haar random unitary. We then take $\psi = \mathcal{U}_{\text{ans}}(\psi_{\text{in}})$ and $\phi = \mathcal{U}_{\text{ans}}(\phi_{\text{in}})$, where \mathcal{U}_{ans} is the unitary for the ansatz circuit in Fig. 11. We compute the expression in (B23) for these random samples ψ and ϕ , and take the maximum value as the tightest lower bound. Note that, since unitaries preserve the orthogonality, such ψ and ϕ always satisfy $D_{\text{tr}}(\psi, \phi) = 1$.

In the main text, we discuss lower bounds with and without bias. A valid lower bound without bias can be obtained by setting $b_A(\psi) = b_A(\phi) = 0$ in the last line of (B23). Recalling that we are focusing on ψ and ϕ with $D_{\text{tr}}(\psi, \phi) = 1$, we get a lower bound without bias with respect to ψ and ϕ as

$$\Delta e_{\text{nobias}}(\psi, \phi) = \frac{1}{D_{\text{tr}}\left(\otimes_{k=1}^K \otimes_{q=1}^Q \mathcal{E}_q^{(k)}(\psi), \otimes_{k=1}^K \otimes_{q=1}^Q \mathcal{E}_q^{(k)}(\phi)\right)}. \quad (\text{E2})$$

For a lower bound with bias, it is convenient to take the third line of (B23) to get

$$\Delta e_{\text{withbias}}(\psi, \phi) = \frac{1 + b_{A^\star}(\psi) - b_{A^\star}(\phi)}{D_{\text{tr}}\left(\otimes_{k=1}^K \otimes_{q=1}^Q \mathcal{E}_q^{(k)}(\psi), \otimes_{k=1}^K \otimes_{q=1}^Q \mathcal{E}_q^{(k)}(\phi)\right)}, \quad (\text{E3})$$

where A^\star is the observable with $-\mathbb{I}/2 \leq A^\star \leq \mathbb{I}/2$ that achieves the trace distance as $\text{Tr}[(A^\star + \mathbb{I}/2)(\psi - \phi)] = D_{\text{tr}}(\psi, \phi) = 1$, which we identify with $A^\star = \psi - \mathbb{I}/2$.